

Clustering by Orthogonal NMF Model and Non-Convex Penalty Optimization

Shuai Wang

*School of Science and Engineering
The Chinese University of Hong Kong, Shenzhen
Shenzhen, 518172, China*

SHUAIWANG@LINK.CUHK.EDU.CN

Tsung-Hui Chang

*School of Science and Engineering
The Chinese University of Hong Kong, Shenzhen
Shenzhen Research Institute of Big Data
Shenzhen, 518172, China*

CHANGTSUNGHUI@CUHK.EDU.CN

Ying Cui

*Department of Industrial and Systems Engineering
University of Southern California
Los Angeles, CA 90089, USA.*

YINGCUI@USC.EDU

Jong-Shi Pang

*Department of Industrial and Systems Engineering
University of Southern California
Los Angeles, CA 90089, USA.*

JONGSHIP@USC.EDU

Abstract

The non-negative matrix factorization (NMF) model with an additional orthogonality constraint on one of the factor matrices, called the orthogonal NMF (ONMF), has been found to provide improved clustering performance over the K-means. Solving the ONMF model is a challenging optimization problem due to the existence of both orthogonality and non-negativity constraints, and most of the existing methods directly deal with the orthogonality constraint in its original form via various optimization techniques. In this paper, we propose a new ONMF based clustering formulation that equivalently transforms the orthogonality constraint into a set of norm-based non-convex equality constraints. We then apply a non-convex penalty (NCP) approach to add the non-convex equality constraints to the objective as penalty terms, leaving simple non-negativity constraints only in the penalized problem. One smooth penalty formulation and one non-smooth penalty formulation are respectively studied, and theoretical conditions for the penalized problems to provide feasible stationary solutions to the ONMF based clustering problem are presented. Experimental results based on both synthetic and real datasets are presented to show that the proposed NCP methods are computationally time efficient, and either match or outperform the existing K-means and ONMF based methods in terms of the clustering performance.

Keywords: Orthogonal NMF, data clustering, penalty method.

1. Introduction

Clustering is one of the most fundamental data mining tasks and has an enormous number of applications (Aggarwal and Reddy, 2013). Typically, clustering is a key intermediate step to explore underlying structure of massive data for subsequent analysis. For example, in internet-based applications, clustering is used to identify group users of different interests who then can be provided with specific service recommendation (Renaud-Deputter et al., 2013; Das et al., 2014). In biology, clustering can be used for pattern discovery of molecular and genes which can help identify subtypes of a certain disease or cancer (Zheng et al., 2009; Brunet et al., 2004; Wang et al., 2018).

Among the existing clustering methods, the K-means (Lloyd, 1982) is the most widely used one, thanks to its simplicity (Ding et al., 2016). However, the K-means may not always yield satisfactory clustering results. On one hand, from an optimization perspective, the iterative steps of finding the cluster centroids and cluster assignment in K-means are equivalent to solving a binary integer constrained matrix factorization problem by alternating optimization (Bauckhage, 2015; Yang et al., 2017a). Due to the non-convex matrix factorization model and binary integer constraint, the iterates of K-means are likely to be stuck in an unsatisfactory local point, and are sensitive to the choice of initial points (Arthur and Vassilvitskii, 2007). On the other hand, the K-means overlooks the inherent low-rank structure and prior information which are usually owned by high-dimensional real data. Therefore, various dimension-reduction techniques such as principal component analysis (PCA), spectral clustering (Luxburg, 2007), non-negative matrix factorization (NMF) (Lee and Seung, 2000; Turkmen, 2015) and deep neural networks (Xie et al., 2016; Yang et al., 2017b) are proposed. However, these methods are merely used as a preprocessing stage to find a low-dimensional, clustering-friendly representation for the data, and the K-means is still often used for clustering the dimension-reduced data. Thus, the intrinsic drawback of the K-means caused by the non-convex and discrete nature of data clustering is not addressed.

Recently, as an variant of NMF, the orthogonal NMF (ONMF) model has been considered for data clustering (Ding et al., 2006; Yoo and Choi, 2010; Choi, 2008; Kimura et al., 2015; Pompili et al., 2014; Asteris et al., 2015; Wang et al., 2018). The ONMF model imposes an additional orthogonality constraint on one of the factor matrices in NMF. It turns out that, like the K-means, the orthogonally constrained factor matrix functions the same as an indicator matrix that shows how the data samples are assigned to different clusters (Ding et al., 2006; Pompili et al., 2014). Therefore, the ONMF model can be regarded as a continuous relaxation (which has no discrete constraint but is still non-convex) of the K-means. Studies on various data mining tasks have found that the ONMF model can outperform the K-means and NMF based clustering methods (Mansour et al., 2014; Mirzal, 2013; Yoo and Choi, 2010; Kimura et al., 2015; Pompili et al., 2014; Asteris et al., 2015; Wang et al., 2018). In addition to data clustering, the ONMF model also shows its popularity in various applications. For instance, the ONMF model is used in (Kim et al., 2010) to capture the principal dynamic activation patterns for generating protein and metabolic sub-networks. The work (Strazar et al., 2016) made use of the ONMF model to discover RNA binding patterns over multiple data to understand protein-RNA interaction. Besides,

reference (Goesele et al., 2010) used the ONMF model to generate discriminative feature representations for object detection.

1.1 Related Works

Despite of its widespread use, solving the ONMF problem is challenging due to the existence of the orthogonality and non-negativity constraints. Many of the existing ONMF algorithms extend upon the classical multiplicative update (MU) rule by Lee and Seung (Lee and Seung, 2000) for the vanilla NMF to accommodate the additional orthogonality constraint. For example, reference (Ding et al., 2006) penalized the orthogonality constraint followed by applying the MU rule. The authors of (Choi, 2008) derived the MU rule directly using the gradient vector over the Stiefel manifold. Reference (Pompili et al., 2014) employed the augmented Lagrangian (AL) method that penalizes the non-negativity constraint and applies the gradient projection method for the orthogonally constrained subproblem. Since projection onto the set of orthonormal matrices involves singular value decomposition (SVD), the orthogonal nonnegatively penalized matrix factorization (ONP-MF) method in (Pompili et al., 2014) can be computationally inefficient. The hierarchical alternating least squares (HALS) method proposed in (Kimura et al., 2015) is claimed to achieve a better balance between the orthogonality and non-negativity constraints. The HALS method updates one column and one row of the two respective factor matrices at the same time in each iteration, subject to the orthogonality and non-negativity constraints. Since the subproblem in HALS is handled by the same MU rule in (Ding et al., 2006), it is computationally efficient in general. Reference (Asteris et al., 2015) proposed to approximate the ONMF solution by solving a low-rank non-negative PCA problem, which however involves generating a large number of candidate solutions. While the method in (Asteris et al., 2015) is the first that can provide provable approximation guarantee for the ONMF problem, it can be computationally inefficient especially when a high-quality solution is sought.

1.2 Contributions

In this paper, we propose a new approach to handle the ONMF based data clustering problem. Specifically, unlike the existing methods (Ding et al., 2006; Kimura et al., 2015; Choi, 2008; Pompili et al., 2014) which directly deal with the orthogonality constraint, we present in (Wang et al., 2019) a novel problem reformulation for the ONMF problem that replaces the orthogonality constraint by a set of norm-based (non-convex) equality constraints. The second ingredient of the proposed approach is the use of the penalty method in optimization (Nocedal and Wright, 2006) to add these non-convex norm-based equality constraints as penalty terms in the objective function. Since only simple non-negativity constraints are left in the penalized problem, it can be efficiently handled by the existing proximal alternating linearized minimization (PALM) method in (Bolte et al., 2014). As will be shown shortly, the proposed algorithms are inherently parallel and therefore are suitable for large-scale clustering problems.

In particular, we consider two types of non-convex penalty (NCP) formulations - one is smooth that has squared ℓ_1 -norm minus squared ℓ_2 -norm as the penalty term, and the other one is non-smooth that has ℓ_1 -norm minus ℓ_∞ -norm as the penalty term. We show that the two penalty methods require different conditions for the penalized problem to yield feasible

and meaningful solutions to the considered ONMF based clustering problem. Specifically, the smooth NCP method yields a feasible solution that satisfies both the orthogonality and non-negativity constraints asymptotically when the penalty parameter goes to infinity, whereas the non-smooth NCP method is an exact penalty method where one can obtain a feasible stationary solution under a finite penalty parameter. These results are new and generalize some of the classical results in (Nocedal and Wright, 2006, Chapter 17).

Extensive experiments are conducted based on a synthetic data set, the document dataset TDT2 (Cai et al., 2011) and the image dataset MNIST (LeCun et al.). The experimental results demonstrate that the proposed NCP methods can provide either comparable or greatly better clustering performance than the existing K-means based and ONMF based methods, while being more time efficient than most of the existing ONMF based methods. It is also shown that the proposed NCP methods are less sensitive to the initial points and the prior knowledge of the number of clusters.

Synopsis: Section 2 reviews the existing K-means and ONMF model, and presents the proposed clustering problem formulation. The proposed NCP optimization framework is presented in Section 3, where theoretical conditions for the smooth and non-smooth NCP methods to yield feasible solutions are analyzed. The PALM algorithms used for solving the smooth and non-smooth penalized problems are given in Section 4. Experimental results are presented in Section 5, and lastly the conclusion is drawn in Section 6.

Notation: We use boldface lowercase letters and boldface uppercase letters to represent column vectors and matrices, respectively. $\mathbb{R}^{m \times n}$ denotes the set of m by n real-valued matrices. The (i, j) th entry of matrix \mathbf{A} is denoted by $[\mathbf{A}]_{ij}$. Superscript T stands for matrix transpose. For a matrix $\mathbf{A} \in \mathbb{R}^{m \times n}$, its column vectors are denoted by \mathbf{a}_j , $j = 1, \dots, n$, and its row vectors are denoted by $\tilde{\mathbf{a}}_i$, $i = 1, \dots, m$; that is,

$$\mathbf{A} = [\mathbf{a}_1, \dots, \mathbf{a}_n] = [\tilde{\mathbf{a}}_1, \dots, \tilde{\mathbf{a}}_m]^T. \quad (1)$$

We denote $\mathbf{A} \in \mathcal{A}^+$ for a non-negative matrix, i.e., $[\mathbf{A}]_{ij} \geq 0$ for all $i = 1, \dots, m, j = 1, \dots, n$. $\mathbf{1}$ denotes the all-one vector, $\mathbf{0}$ is the all-zero vector, \mathbf{I}_m is the m by m identity matrix, and \mathbf{e}_n denotes the elementary vector with one in the n th entry and zero otherwise. $\|\cdot\|_F$ and $\|\cdot\|_p$ are the matrix Frobenius norm and vector p-norm, respectively. $\langle \mathbf{A}, \mathbf{B} \rangle$ denotes the inner product between matrices \mathbf{A} and \mathbf{B} . $\lambda_{\max}(\mathbf{A})$ stands for the maximum eigenvalue of matrix \mathbf{A} . For a convex function $f: \mathbb{R}^n \rightarrow \mathbb{R}$, $\partial f(\mathbf{x})$ denotes the subdifferential of f at \mathbf{x} .

2. ONMF based Data Clustering

2.1 K-Means and ONMF Model

Let $\mathbf{X} \in \mathcal{X}^+$ be a non-negative data matrix that contains N data samples and each of the samples has M features, i.e., $\mathbf{X} = [\mathbf{x}_1, \dots, \mathbf{x}_N] \in \mathbb{R}^{M \times N}$. The task of data clustering is to assign the N data samples into a predefined number of K clusters in the sense that the samples belonging to one cluster are close to each other based on certain distance metric (Theodoridis and Koutroumbas, 2008). The most popular setting is to consider the Euclidean distance and the use of the K-means due to its simplicity.

From an optimization point of view (Bauckhage, 2015; Yang et al., 2017a), the K-means can be interpreted as an alternating optimization algorithm applied to the following matrix

factorization problem

$$\min_{\mathbf{W}, \mathbf{H}} \|\mathbf{X} - \mathbf{W}\mathbf{H}\|_F^2, \quad (2a)$$

$$\text{s.t. } \mathbf{1}^T \mathbf{h}_j = 1, [\mathbf{H}]_{ij} \in \{0, 1\}, \forall i \in \mathcal{K}, j \in \mathcal{N}, \quad (2b)$$

$$\mathbf{W} \in \mathcal{W}^+, \quad (2c)$$

where $\mathcal{K} \triangleq \{1, \dots, K\}$ and $\mathcal{N} \triangleq \{1, \dots, N\}$. Here, columns of $\mathbf{W} \in \mathbb{R}^{M \times K}$ represent centroids of the K clusters, while the matrix $\mathbf{H} \in \mathbb{R}^{K \times N}$ indicates the cluster assignment of samples. Specifically, $[\mathbf{H}]_{ij} = 1$ if the j th sample is uniquely assigned to cluster i , and $[\mathbf{H}]_{ij} = 0$ otherwise.

One can see from (2) that, when \mathbf{W} is given, the optimal \mathbf{H} is obtained by assigning each sample to the cluster that has the nearest centroid, while when \mathbf{H} is given, the optimal \mathbf{W} is given by the centroids of K clusters. The two steps are exactly the well-known K-means algorithm. However, due to the non-convex binary constraint (2b), the K-means is sensitive to the initial conditions and may not always yield satisfactory clustering performance. Therefore, there have been efforts to finding a better initial point for the K-means; see, e.g., the K-means++ (Arthur and Vassilvitskii, 2007).

Regarded as a relaxation of (2), the following vanilla NMF model is also considered for data clustering (Turkmen, 2015; Pompili et al., 2014; Yang et al., 2017a)

$$\min_{\mathbf{W}, \mathbf{H}} \|\mathbf{X} - \mathbf{W}\mathbf{H}\|_F^2 \quad (3a)$$

$$\text{s.t. } \mathbf{W} \in \mathcal{W}^+, \mathbf{H} \in \mathcal{H}^+. \quad (3b)$$

However, the obtained \mathbf{H} usually does not reveal clear clustering assignment, and thus additional clustering step (such as K-means or hierarchical clustering) is needed and applied to \mathbf{H} .

It was shown in (Ding et al., 2006; Pompili et al., 2014) that the ONMF model, which has an additional orthogonality constraint on \mathbf{H} , is closely related to the K-means model (2). In particular, the ONMF problem is given by

$$\min_{\mathbf{W}, \mathbf{H}} \|\mathbf{X} - \mathbf{W}\mathbf{H}\|_F^2 \quad (4a)$$

$$\text{s.t. } \mathbf{W} \in \mathcal{W}^+, \mathbf{H} \in \mathcal{H}^+, \quad (4b)$$

$$\mathbf{H}\mathbf{H}^T = \mathbf{I}_K. \quad (4c)$$

A key observation is given as below.

Observation: Any \mathbf{H} satisfying $\mathbf{H} \in \mathcal{H}^+$ and $\mathbf{H}\mathbf{H}^T = \mathbf{I}_K$ has at most one non-zero entry in each column.

Thus, matrix \mathbf{H} in (4) functions similarly as that in (2) and indicates the cluster assignment of data samples. Nevertheless, different from (2), the non-zero entries of \mathbf{H} in (4) are not restricted to be one but can be scaled. Owing to the two facts, the ONMF model is less sensitive to data scaling and may outperform the K-means and vanilla NMF model (Turkmen, 2015; Pompili et al., 2014; Yang et al., 2017a).

However, the ONMF problem (4) is challenging to solve in general. Unlike the existing methods (Ding et al., 2006; Kimura et al., 2015; Choi, 2008; Pompili et al., 2014) which directly deal with the orthogonality constraint (4c), we present a novel problem reformulation of (4) and propose a non-convex penalty (NCP) optimization method that is not only amenable to efficient computation but also able to provide favorable clustering performance.

2.2 Proposed Clustering Formulation

Since any vector $\mathbf{x} \in \mathbb{R}^n$ has at most one non-zero entry if and only if

$$\|\mathbf{x}\|_p = \|\mathbf{x}\|_q, \quad 1 \leq p < q, \quad (5)$$

according to the Observation, any \mathbf{H} satisfying (4c) and (4b) also lies in the following set

$$\left\{ \mathbf{H} \in \mathcal{H}^+ \mid \begin{array}{l} \|\tilde{\mathbf{h}}_i\|_2 = 1, \quad i \in \mathcal{K}, \\ \|\mathbf{h}_j\|_p = \|\mathbf{h}_j\|_q, \quad j \in \mathcal{N} \end{array} \right\}. \quad (6)$$

Thus, the ONMF model (4) can be equivalently written as

$$\min_{\mathbf{W}, \mathbf{H}} \|\mathbf{X} - \mathbf{WH}\|_F^2 \quad (7a)$$

$$\text{s.t. } \mathbf{W} \in \mathcal{W}^+, \mathbf{H} \in \mathcal{H}^+, \quad (7b)$$

$$\|\tilde{\mathbf{h}}_i\|_2 = 1, \quad i \in \mathcal{K}, \quad (7c)$$

$$\|\mathbf{h}_j\|_p = \|\mathbf{h}_j\|_q, \quad j \in \mathcal{N}. \quad (7d)$$

Firstly, note that the condition $\|\tilde{\mathbf{h}}_i\|_2 = 1, i \in \mathcal{K}$, is not intrinsic to the data clustering task. In essence, both \mathbf{H} and \mathbf{QH} , where $\mathbf{Q} \geq 0$ is a diagonal matrix, indicate the same cluster assignment, and both (\mathbf{W}, \mathbf{H}) and $(\mathbf{WQ}^{-1}, \mathbf{QH})$ have the same objective values in (7a). Therefore, without loss of the clustering performance, we remove $\|\tilde{\mathbf{h}}_i\|_2 = 1, i \in \mathcal{K}$, from (7). Secondly, for bounded solution, we add the regularization term $\frac{\mu}{2}\|\mathbf{W}\|_F^2 + \frac{\nu}{2}\|\mathbf{H}\|_F^2$ to (7), where $\mu, \nu \geq 0$ are two parameters¹. Thirdly, without loss of generality, we replace $\|\mathbf{h}_j\|_p = \|\mathbf{h}_j\|_q$ with $\|\mathbf{h}_j\|_p^v = \|\mathbf{h}_j\|_q^v$ by adding a power exponent $v > 0$. As a result, we have the following problem formulation for data clustering:

Proposed clustering formulation:

$$\min_{\mathbf{W}, \mathbf{H}} \|\mathbf{X} - \mathbf{WH}\|_F^2 + \frac{\mu}{2}\|\mathbf{W}\|_F^2 + \frac{\nu}{2}\|\mathbf{H}\|_F^2 \quad (8a)$$

$$\text{s.t. } \mathbf{W} \in \mathcal{W}^+, \quad (8b)$$

$$\left. \begin{array}{l} \mathbf{H} \in \mathcal{H}^+, \\ \|\mathbf{h}_j\|_p^v = \|\mathbf{h}_j\|_q^v, \quad j \in \mathcal{N}, \end{array} \right\} \triangleq \mathcal{H}_{p,q}^v. \quad (8c)$$

One clear advantage of formulation (8) is its scalability. Concisely, when \mathbf{W} is fixed, problem (8) can be fully decoupled across the columns of \mathbf{H} into N subproblems. This

1. Adding the regularization term makes the objective coercive, which subsequently can guarantee bounded solutions to the optimization problem. Alternatively, one can obtain bounded \mathbf{W} and \mathbf{H} by imposing some box constraints. Either way is fine to the proposed methods developed in Section 3 and Section 4.

makes it easy to apply some decomposition methods for dealing with large-scale clustering tasks. Nevertheless, it is still challenging to solve (8) and the main challenge lies in how to deal with the non-convex objective function and the (possibly non-smooth) norm-equality constraint (8c).

Before proceeding with the proposed methods, we first present some basic definitions in order to characterize a stationary solution of the non-convex and possibly non-smooth optimization problem (8).

Definition 1 (*Tangent cone*) (Facchinei and Pang, 2003, Sec. 1.3.1) Let $\mathcal{X} \subseteq \mathbb{R}^n$ and $\mathbf{x} \in \mathcal{X}$. A vector \mathbf{d} is a tangent of \mathcal{X} at \mathbf{x} if either $\mathbf{d} = \mathbf{0}$ or there exists a sequence $\{\mathbf{x}^k\} \subset \mathcal{X}$ and positive scalars $\{\tau^k\}$ such that when $\mathbf{x}^k \rightarrow \mathbf{x}$, $\tau^k \searrow 0$,

$$\lim_{k \rightarrow \infty} \frac{\mathbf{x}^k - \mathbf{x}}{\tau^k} = \mathbf{d}. \quad (9)$$

The tangent cone of \mathcal{X} at \mathbf{x} , denoted by $\mathcal{T}_{\mathcal{X}}(\mathbf{x})$, contains all the tangents of \mathcal{X} at \mathbf{x} .

Definition 2 (*Directional derivative*) (Pang et al., 2017, Sec. 3.1) Let $f : \mathbb{R}^n \rightarrow \mathbb{R}$ be a possibly non-smooth function. Then f is directionally differentiable if the directional derivative of f along any direction $\mathbf{d} \in \mathbb{R}^n$

$$f'(\mathbf{x}; \mathbf{d}) = \lim_{\tau \searrow 0} \frac{f(\mathbf{x} + \tau \mathbf{d}) - f(\mathbf{x})}{\tau} \quad (10)$$

exists at any $\mathbf{x} \in \mathbb{R}^n$.

Definition 3 (*B-stationary solution*) (Pang et al., 2017, Eqn. (18)) For an optimization problem $\min_{\mathbf{x} \in \mathcal{X}} f(\mathbf{x})$, where $f : \mathbb{R}^n \rightarrow \mathbb{R}$ is possibly non-smooth but directionally differentiable, and \mathcal{X} is a closed set. Then, $\bar{\mathbf{x}} \in \mathcal{X}$ is a B-stationary point if $f'(\bar{\mathbf{x}}; \mathbf{d}) \geq 0, \forall \mathbf{d} \in \mathcal{T}_{\mathcal{X}}(\bar{\mathbf{x}})$.

If f is differentiable, then the directional derivative $f'(\bar{\mathbf{x}}; \mathbf{d})$ in the above condition can be replaced by $\nabla f(\bar{\mathbf{x}})^T \mathbf{d}$. If \mathcal{X} is a convex set, then the condition is equivalent to $f'(\bar{\mathbf{x}}; \mathbf{x} - \bar{\mathbf{x}}) \geq 0, \forall \mathbf{x} \in \mathcal{X}$, and $\bar{\mathbf{x}}$ is known as the *d-stationary point*. If f is differentiable and \mathcal{X} is convex, then the condition reduces to $\nabla f(\bar{\mathbf{x}})^T (\mathbf{x} - \bar{\mathbf{x}}) \geq 0, \forall \mathbf{x} \in \mathcal{X}$, and $\bar{\mathbf{x}}$ is simply called a *stationary point* (Facchinei and Pang, 2003, (1.3.3)).

The following simple proposition shows that any B-stationary point of (8) has non-zero columns for \mathbf{H} , implying that each data sample must be assigned to one of the clusters.

Proposition 1 Let $(\bar{\mathbf{W}}, \bar{\mathbf{H}})$ be a B-stationary point of (8) satisfying $(\bar{\mathbf{W}})^T \mathbf{x}_j \neq \mathbf{0}, \forall j \in \mathcal{N}$. Then, $\bar{\mathbf{h}}_j \neq \mathbf{0}, \forall j \in \mathcal{N}$.

Proof: Since $(\bar{\mathbf{W}}, \bar{\mathbf{H}})$ is a B-stationary point of (8), we have

$$\langle 2(\bar{\mathbf{W}})^T (\bar{\mathbf{W}} \bar{\mathbf{H}} - \mathbf{X}) + \nu \bar{\mathbf{H}}, \mathbf{D} \rangle \geq 0, \forall \mathbf{D} \in \mathcal{T}_{\mathcal{H}_{p,q}^{\nu}}(\bar{\mathbf{H}}). \quad (11)$$

Suppose that there exist $j' \in \mathcal{N}$ such that $\bar{\mathbf{h}}_{j'} = \mathbf{0}$. Then, (11) becomes

$$\sum_{j \neq j'} \langle 2(\bar{\mathbf{W}})^T (\bar{\mathbf{W}} \bar{\mathbf{h}}_j - \mathbf{x}_j) + \nu \bar{\mathbf{h}}_j, \mathbf{d}_j \rangle - \langle 2(\bar{\mathbf{W}})^T \mathbf{x}_{j'}, \mathbf{d}_{j'} \rangle \geq 0, \quad \forall \mathbf{D} \in \mathcal{T}_{\mathcal{H}_{p,q}^v}(\bar{\mathbf{H}}). \quad (12)$$

Suppose that $((\bar{\mathbf{W}})^T \mathbf{x}_{j'})_\ell > 0$ for some $\ell \in \mathcal{K}$. Choose a direction $\bar{\mathbf{D}}$ such that $\bar{\mathbf{d}}_j = \mathbf{0}, \forall j \neq j', \bar{\mathbf{d}}_{j'} = \alpha \mathbf{e}_\ell$ for some $\alpha > 0$. It is obvious to see that $\bar{\mathbf{D}} \in \mathbf{T}_{\mathcal{H}_{p,q}^v}(\bar{\mathbf{H}})$ based on Definition 1. By substituting $\bar{\mathbf{D}}$ into (12), we obtain

$$0 > -2 \langle (\bar{\mathbf{W}})^T \mathbf{x}_{j'}, \alpha \mathbf{e}_\ell \rangle = -2\alpha ((\bar{\mathbf{W}})^T \mathbf{x}_{j'})_\ell \geq 0, \quad (13)$$

which, however, is a contradiction. \blacksquare

The condition of $(\bar{\mathbf{W}})^T \mathbf{x}_j \neq \mathbf{0}, \forall j \in \mathcal{N}$, in Proposition 1 is actually mild as it is known that the centroid \mathbf{W} should usually lie in the space spanned by the cluster samples (Ding et al., 2010).

3. Proposed Non-Convex Penalty Methods

In this section, we present the proposed NCP framework to handle problem (8). Specifically, since $\phi(\mathbf{h}_j) \triangleq \|\mathbf{h}_j\|_p^v - \|\mathbf{h}_j\|_q^v \geq 0$ for $1 \leq p < q$, we consider the following penalized formulation

$$\min_{\mathbf{W}, \mathbf{H}} F(\mathbf{W}, \mathbf{H}) + \frac{\rho}{v} \sum_{j=1}^N \left(\|\mathbf{h}_j\|_p^v - \|\mathbf{h}_j\|_q^v \right) \quad (14a)$$

$$\text{s.t. } \mathbf{W} \in \mathcal{W}^+, \mathbf{H} \in \mathcal{H}^+, \quad (14b)$$

where $F(\mathbf{W}, \mathbf{H}) \triangleq \|\mathbf{X} - \mathbf{W}\mathbf{H}\|_F^2 + \frac{\mu}{2} \|\mathbf{W}\|_F^2 + \frac{\nu}{2} \|\mathbf{H}\|_F^2$, and $\rho > 0$ is a penalty parameter. As seen from (14), since the non-convex norm-equality constraints in (8c) are penalized in the objective function, the penalized problem (14) involves simple convex constraint set only.

Like the classical penalty method (Nocedal and Wright, 2006, Chapter 17), we attempt to reach a good clustering solution of (8) through solving a sequence of penalized sub-problems in (14), by gradually increasing ρ . The proposed NCP framework is shown in Algorithm 1.

Algorithm 1 Proposed NCP framework for problem (8).

- 1: **Set** $r = 1$, and given a parameter $\gamma > 1$ and initial values of $\rho > 0$ and $(\mathbf{W}^{(0)}, \mathbf{H}^{(0)})$.
 - 2: **repeat**
 - 3: Obtain a d-stationary point $(\mathbf{W}^{(r)}, \mathbf{H}^{(r)})$ of problem (14), using $(\mathbf{W}^{(r-1)}, \mathbf{H}^{(r-1)})$ as the initial point (see Algorithm 2 and Algorithm 3 in Section 4).
 - 4: Increase the penalty parameter $\rho = \gamma\rho$ if the row vectors of $\mathbf{H}^{(r)}$ are not sufficiently orthogonal (see Section 5).
 - 5: Set $r = r + 1$.
 - 6: **until** a predefined stopping criteria is satisfied.
-

We study two types of penalty functions. In particular, we respectively consider a smooth penalty and a non-smooth penalty for (14). The smooth penalty sets $p = 1$, $q = 2$ and $v = 2$, whereas the non-smooth penalty sets $p = 1$, $q = \infty$ and $v = 1$. In the ensuing two subsections, we present theoretical conditions for which the penalty method and Algorithm 1 can yield a feasible and B-stationary solution to problem (8).

3.1 Smooth NCP Method

The proposed smooth NCP is obtained by choosing $p = 1$, $q = 2$ and $v = 2$ in (8) and (14). Since $\mathbf{H} \in \mathcal{H}^+$, $\|\mathbf{h}_j\|_1 = \mathbf{1}^T \mathbf{h}_j$, $j \in \mathcal{N}$, the corresponding penalized problem (14) is given by

$$\min_{\mathbf{W}, \mathbf{H}} F(\mathbf{W}, \mathbf{H}) + \frac{\rho}{2} \sum_{j=1}^N \left((\mathbf{1}^T \mathbf{h}_j)^2 - \|\mathbf{h}_j\|_2^2 \right) \quad (15a)$$

$$\text{s.t. } \mathbf{W} \in \mathcal{W}^+, \mathbf{H} \in \mathcal{H}^+, \quad (15b)$$

which has $G_\rho(\mathbf{W}, \mathbf{H}) \triangleq F(\mathbf{W}, \mathbf{H}) + \frac{\rho}{2} \sum_{j=1}^N \left((\mathbf{1}^T \mathbf{h}_j)^2 - \|\mathbf{h}_j\|_2^2 \right)$ as the differentiable objective function.

One of the most fundamental questions regarding the penalty method is whether the penalized problem (15) can yield a solution (\mathbf{W}, \mathbf{H}) that is also a feasible and meaningful solution to the original problem (8). The proposition below shows that the answer is positive provided that one can reach a local minimum point of problem (15).

Proposition 2 *Let $(\mathbf{W}^*, \mathbf{H}^*)$ be a local minimizer of problem (15). Then the following assertions hold.*

- (a) *If $\mu = 0$ in (8) and (15), then for any $\rho > 0$, $(\mathbf{W}^*, \mathbf{H}^*)$ is feasible and a local minimizer to (8).*
- (b) *For $\mu > 0$, there exists a finite ρ^* such that for any $\rho > \rho^*$, $(\mathbf{W}^*, \mathbf{H}^*)$ is feasible and a local minimizer to (8).*

The proof of Proposition 2 is given in Appendix A. While Proposition 2 is encouraging, problem (15) is non-convex and therefore a local minimum solution cannot be computed in general. Instead, most of the non-convex optimization algorithms can only guarantee a stationary point under proper conditions (Bertsekas, 1999).

Let us denote $(\mathbf{W}^\rho, \mathbf{H}^\rho)$ as a stationary point of (15), and assume that $(\mathbf{W}^\rho, \mathbf{H}^\rho)$ is bounded and it has a limit point $(\mathbf{W}^\infty, \mathbf{H}^\infty)$ when $\rho \rightarrow \infty$. We have the following theorem.

Theorem 1 *(a) $(\mathbf{W}^\infty, \mathbf{H}^\infty)$ is feasible to (8), and (b) if the Mangasarian-Fromovitz constraint qualification (MFCQ) (Facchinei and Pang, 2003, Sec. 3.2) holds for (8) at $(\mathbf{W}^\infty, \mathbf{H}^\infty)$, then $(\mathbf{W}^\infty, \mathbf{H}^\infty)$ is a B-stationary point of (8).*

The proof of Theorem 1 is presented in Appendix B. Theorem 1(a) implies that by solving the penalized problem (15) to a stationary solution sequentially with increased ρ , one eventually can obtain a feasible (\mathbf{W}, \mathbf{H}) for (8). Besides, as shown in Theorem 1(b),

the obtained solution will asymptotically be a B-stationary point of the original problem (8), as long as the MFCQ holds.

Surprisingly, for problem (8), MFCQ can never hold for the feasible $(\mathbf{W}^\infty, \mathbf{H}^\infty)$. To see this, denote $\phi_j(\mathbf{H}) = (\mathbf{1}^T \mathbf{h}_j)^2 - \|\mathbf{h}_j\|_2^2$, $j \in \mathcal{N}$. Then the MFCQ for (8) correspond to the following conditions

- 1) $\nabla \phi_j(\mathbf{H}^\infty)$, $j = 1, \dots, N$, are linearly independent;
- 2) there exists \mathbf{D} satisfying

$$\langle \nabla_{\mathbf{H}} \phi_j(\mathbf{H}^\infty), \mathbf{D} \rangle = 0, \forall j \in \mathcal{N}, \quad (16)$$

$$[\mathbf{D}]_{i,j} > 0, \text{ if } [\mathbf{H}^\infty]_{i,j} = 0. \quad (17)$$

Since

$$[\nabla_{\mathbf{H}} \phi_j(\mathbf{H}^\infty)]_{i,j'} = \begin{cases} 2\mathbf{1}^T \mathbf{h}_{j'}^\infty, & \text{if } j' = j \text{ and } [\mathbf{H}^\infty]_{i,j'} = 0, \\ 0, & \text{otherwise,} \end{cases} \quad (18)$$

it is obvious that $\nabla_{\mathbf{H}} \phi_j(\mathbf{H}^\infty)$, $j = 1, \dots, N$, are linearly independent. However, by (18) and (17), we have

$$\langle \nabla_{\mathbf{H}} \phi_j(\mathbf{H}^\infty), \mathbf{D} \rangle = \sum_{i=1}^K [\nabla_{\mathbf{H}} \phi_j(\mathbf{H}^\infty)]_{i,j} [\mathbf{D}]_{i,j} > 0, \quad (19)$$

which violates (16), and thereby the MFCQ does not hold for $(\mathbf{W}^\infty, \mathbf{H}^\infty)$. Nevertheless, we should emphasize that Theorem 1(b) is only a sufficient condition for obtaining a B-stationary point of (8), and the smooth NCP method may still perform well in practice. In fact, experimental results presented in Section 5 will show that the smooth NCP method can yield promising clustering performance for both synthetic and real data sets under our test.

3.2 Non-smooth NCP method

In this subsection, we consider a non-smooth NCP method by setting $p = 1$, $q = \infty$ and $v = 1$ in (8) and (14). The corresponding penalized problem (14) is given by

$$\min_{\mathbf{W}, \mathbf{H}} F(\mathbf{W}, \mathbf{H}) + \rho \sum_{j=1}^N (\mathbf{1}^T \mathbf{h}_j - \|\mathbf{h}_j\|_\infty) \quad (20a)$$

$$\text{s.t. } \mathbf{W} \in \mathcal{W}^+, \mathbf{H} \in \mathcal{H}^+, \quad (20b)$$

where the objective function $F_\rho(\mathbf{W}, \mathbf{H}) \triangleq F(\mathbf{W}, \mathbf{H}) + \rho \sum_{j=1}^N (\mathbf{1}^T \mathbf{h}_j - \|\mathbf{h}_j\|_\infty)$ is non-smooth. Interestingly, in contrast to Theorem 1, the non-smooth NCP method allows one to obtain a feasible B-stationary solution of (8) under a finite ρ .

Theorem 2 *For any bounded set \mathcal{B} , there exists a finite $\rho^* > 0$ such that for all $\rho > \rho^*$, if $(\mathbf{W}^\rho, \mathbf{H}^\rho) \in \mathcal{B}$ is a d -stationary point of (20), then the following assertions hold.*

- (a) $(\mathbf{W}^\rho, \mathbf{H}^\rho)$ is feasible to (8).

(b) $(\mathbf{W}^\rho, \mathbf{H}^\rho)$ is a B -stationary point to (8).

The proof of Theorem 2 is presented in Appendix D. In contrast to Theorem 1, Theorem 2 suggests that Algorithm 1 using the non-smooth penalized problem (20) may be able to reach a feasible solution of (8) in a pace faster than that using its smooth counterpart in (15), and is less sensitive to the choice of penalty parameter ρ (Nocedal and Wright, 2006). However, this does not imply that the non-smooth NCP method can be more time-efficient or can provide better clustering performance than the smooth NCP method. This is because the non-smooth penalized problem (20) is in general more challenging to solve than the smooth problem (15). Besides, the two problems (20) and (15) may yield different stationary points, depending on the solvers employed. Interesting comparison between the smooth and non-smooth NCP methods will be further discussed in Section 5.

4. Obtaining a Stationary Point of (14)

In this section, we present algorithms that can be used to obtain a proper stationary solution of the penalized problems (15) and (20). In view of the separable constraint structure for \mathbf{W} and \mathbf{H} , the PALM algorithm in (Bolte et al., 2014) is particularly efficient in handling the considered penalized problems. Specifically, by applying the PALM algorithm to the smooth penalized problems (15), one simply performs block-wise gradient projection with respect to \mathbf{W} and \mathbf{H} iteratively, as shown in Algorithm 2. Here, t^k and c^k are two step size parameters. Denote $L_G(\mathbf{W}^k)$ and $L_G(\mathbf{H}^k)$ as the Lipschitz constant of $\nabla_{\mathbf{H}}G_\rho(\mathbf{W}^k, \mathbf{H}^k)$ and $\nabla_{\mathbf{W}}G_\rho(\mathbf{W}^k, \mathbf{H}^k)$, respectively. Convergence of Algorithm 2 has been established in (Bolte et al., 2014).

Theorem 3 (Bolte et al., 2014) *Let $\{\mathbf{W}^k, \mathbf{H}^k\}$ be the sequence generated by Algorithm 2 with $t^k > \frac{L_G(\mathbf{W}^k)}{2}$ and $c^k > \frac{L_G(\mathbf{H}^k)}{2}$. Then $\{G_\rho(\mathbf{W}^k, \mathbf{H}^k)\}$ is non-increasing, $\{\mathbf{W}^k, \mathbf{H}^k\}$ is bounded, and $\{\mathbf{W}^k, \mathbf{H}^k\}$ converges to a stationary point of (15).*

Proof: Since $G_\rho(\mathbf{W}, \mathbf{H})$ is a coercive function, and the PALM updates in Algorithm 2 guarantees descent of the objective function $G_\rho(\mathbf{W}^k, \mathbf{H}^k)$ (Bolte et al., 2014, Remark 4(iii)) under $t^k > \frac{L_G(\mathbf{W}^k)}{2}$ and $c^k > \frac{L_G(\mathbf{H}^k)}{2}$, $\{\mathbf{W}^k, \mathbf{H}^k\}$ are bounded. Besides, because $G_\rho(\mathbf{W}, \mathbf{H})$ satisfies the Kurdyka-Lojasiewicz (KL) property, and \mathcal{W}^+ , \mathcal{H}^+ are convex sets, we can obtain the desired results by Bolte et al. (2014, Theorem 1). \blacksquare

Algorithm 2 PALM for solving penalized problem (15).

- 1: **Set** $k = 0$, $\mathbf{W}^0 = \mathbf{W}^{(r-1)}$, $\mathbf{H}^0 = \mathbf{H}^{(r-1)}$.
 - 2: **repeat**
 - 3: $\mathbf{H}^{k+1} = \max \left\{ \mathbf{H}^k - \frac{1}{t^k} \nabla_{\mathbf{H}} G_\rho(\mathbf{W}^k, \mathbf{H}^k), 0 \right\}$,
 $\mathbf{W}^{k+1} = \max \left\{ \mathbf{W}^k - \frac{1}{c^{k+1}} \nabla_{\mathbf{W}} G_\rho(\mathbf{W}^k, \mathbf{H}^{k+1}), 0 \right\}$,
 - 4: Set $k = k + 1$,
 - 5: **until** a predefined stopping criteria is satisfied.
-

For the non-smooth penalized problem (20), we apply the same PALM principle but replace the gradient by the subgradient for the update of \mathbf{H} . For example, one such choice

is given by

$$\nabla_{\mathbf{H}}\tilde{F}(\mathbf{W}, \mathbf{H}) - \rho\mathbf{E} \in \partial_{\mathbf{H}}F_{\rho}(\mathbf{W}, \mathbf{H}), \quad (21)$$

where $\tilde{F}(\mathbf{W}, \mathbf{H}) \triangleq F(\mathbf{W}, \mathbf{H}) + \rho \sum_{j=1}^N \mathbf{1}^T \mathbf{h}_j$, $\mathbf{E} = [\mathbf{e}_{i_1}, \mathbf{e}_{i_2}, \dots, \mathbf{e}_{i_N}]$, $i_j \in \arg \max_{i=1, \dots, K} [\mathbf{H}]_{ij}$ and $\mathbf{e}_{i_j} \in \partial \|\mathbf{h}_j\|_{\infty}$. The algorithm is shown in Algorithm 3. Let $L_{\tilde{F}}(\mathbf{W}^k)$ and $L_F(\mathbf{H}^k)$ as the Lipschitz constant of $\nabla_{\mathbf{H}}\tilde{F}(\mathbf{W}^k, \mathbf{H})$ and $\nabla_{\mathbf{W}}F_{\rho}(\mathbf{W}, \mathbf{H}^k)$, respectively.

Theorem 4 *Let $\{\mathbf{W}^k, \mathbf{H}^k\}$ be the sequence generated by Algorithm 3 with $t^k > \frac{L_{\tilde{F}}(\mathbf{W}^k)}{2}$ and $c^k > \frac{L_F(\mathbf{H}^k)}{2}$. Then $\{F_{\rho}(\mathbf{W}^k, \mathbf{H}^k)\}$ is non-increasing, $\{\mathbf{W}^k, \mathbf{H}^k\}$ is bounded, and $\{\mathbf{W}^k, \mathbf{H}^k\}$ converges to a stationary point of (20) satisfying*

$$\begin{aligned} \langle \nabla_{\mathbf{H}}\tilde{F}(\mathbf{W}, \mathbf{H}) - \rho\mathbf{E}, \mathbf{D} \rangle + \langle \nabla_{\mathbf{W}}F_{\rho}(\mathbf{W}, \mathbf{H}), \mathbf{S} \rangle \geq 0, \\ \forall \mathbf{D} \in \mathcal{T}_{\mathcal{H}^+}(\mathbf{H}), \mathbf{S} \in \mathcal{T}_{\mathcal{W}^+}(\mathbf{W}). \end{aligned} \quad (22)$$

Proof: The proof can be obtained by following the same idea as proving Bolte et al. (2014, Theorem 1) and Theorem 3. However, since Bolte et al. (2014) has assumed convex non-smooth terms in the objective but we have concave non-smooth term $-\sum_{j=1}^N \|\mathbf{h}_j\|_{\infty}$ in (20), we need extend the sufficient decrease property in (Bolte et al., 2014, Lemma 2) to show that the update of \mathbf{H} in Algorithm 3 enjoys the same descent property. This is presented in Appendix E. \blacksquare

Algorithm 3 PALM for solving penalized problem (20).

- 1: **Set** $k = 0$, $\mathbf{W}^0 = \mathbf{W}^{(r-1)}$, $\mathbf{H}^0 = \mathbf{H}^{(r-1)}$.
 - 2: **repeat**
 - 3: $\mathbf{H}^{k+1} = \max \left\{ \mathbf{H}^k - \frac{1}{t^k} (\nabla_{\mathbf{H}}\tilde{F}(\mathbf{W}^k, \mathbf{H}^k) - \rho\mathbf{E}^k), 0 \right\}$,
 $\mathbf{W}^{k+1} = \max \left\{ \mathbf{W}^k - \frac{1}{c^{k+1}} \nabla_{\mathbf{W}}F_{\rho}(\mathbf{W}^k, \mathbf{H}^{k+1}), 0 \right\}$,
 - 4: Set $k = k + 1$,
 - 5: **until** a predefined stopping criteria is satisfied.
-

5. Experiment Results

In this section, we examine the clustering performance of the proposed smooth NCP (SNCP) and non-smooth NCP (NSNCP) methods against six existing clustering methods, namely, K-means (KM), K-means++ (Arthur and Vassilvitskii, 2007), DTPP (Ding et al., 2006), ONP-MF (Pompili et al., 2014), ONMF-S (Choi, 2008) and HALS (Kimura et al., 2015). Note that the later four methods are all based on the ONMF model (4). The adjusted Rand index (ARI) (Yeung and Ruzzo, 2001) and clustering accuracy (ACC) (Cai et al., 2011) are adopted for performance evaluation.

5.1 Performance with Synthetic Data

The synthetic data is generated by the linear model $\mathbf{X} = \mathbf{W}\mathbf{H} + \mathbf{V}$ where $\mathbf{V} \in \mathbb{R}^{M \times N}$ denotes the measurement noise. The signal to noise ratio (SNR) is defined as $10 \log_{10}(\|\mathbf{W}\mathbf{H}\|_F^2 / \|\mathbf{V}\|_F^2)$

dB. We follow the same procedure as in (Yang et al., 2017a) to generate \mathbf{W} , \mathbf{V} and the cluster assignment matrix \mathbf{H} , with $M = 2000$, $N = 1000$ and $K = 10$ (ten clusters). The number of data samples in the 10 clusters are 117, 62, 36, 124, 15, 24, 119, 43, 122 and 338, respectively. Like Yang et al. (2017a), 5% of the data samples are replaced by randomly generated outliers.

Parameter setting: We choose $\nu = 10^{-4}$ and $\mu = 0$ in (8). In Algorithm 1, the initial penalty parameter ρ is set to 10^{-8} and the parameter γ for increasing ρ is set to 1.1. For Step 4 of Algorithm 1, the orthogonality of $\mathbf{H}^{(r)}$ is measured by

$$\text{(Orthogonality)} \ \epsilon_{\text{orth}} = \frac{\|\mathbf{Q}^{(r)}\mathbf{H}^{(r)}(\mathbf{Q}^{(r)}\mathbf{H}^{(r)})^T - \mathbf{I}_K\|_F}{K^2}, \quad (23)$$

where $\mathbf{Q}^{(r)}$ is a diagonal matrix such that rows of $\mathbf{Q}^{(r)}\mathbf{H}^{(r)}$ have unit 2-norm. One updates $\rho = \gamma\rho$ in Step 4 of Algorithm 1 if $\epsilon_{\text{orth}} \geq 10^{-10}$. Besides, we define

$$\text{(Normalized Residual)} \ \epsilon_{\text{NR}} = \frac{\|\mathbf{W}^{(r)} - \mathbf{W}^{(r-1)}\|_F}{\|\mathbf{W}^{(r-1)}\|_F} + \frac{\|\mathbf{H}^{(r)} - \mathbf{H}^{(r-1)}\|_F}{\|\mathbf{H}^{(r-1)}\|_F}. \quad (24)$$

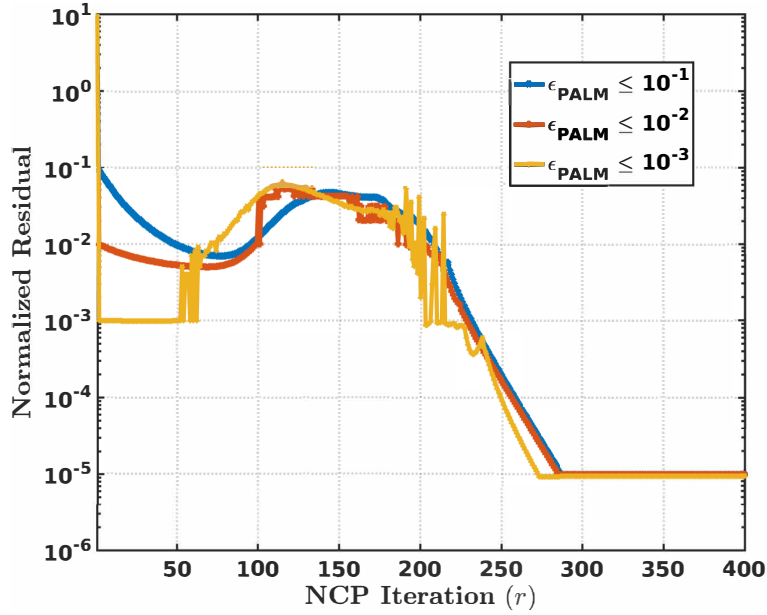
The stopping condition of Algorithm 1 is when both ϵ_{orth} and ϵ_{NR} are sufficiently small.

For Algorithm 2, t^k and c^{k+1} are chosen as $\frac{1}{2}\lambda_{\max}(\nabla_{\mathbf{H}}^2 G_{\rho}(\mathbf{W}^k, \mathbf{H}^k))$ and $\frac{1}{2}\lambda_{\max}(\nabla_{\mathbf{W}}^2 G_{\rho}(\mathbf{W}^k, \mathbf{H}^{k+1}))$, respectively; while for Algorithm 3, t^k and c^{k+1} are chosen as $\frac{1}{2}\lambda_{\max}(\nabla_{\mathbf{H}}^2 \tilde{F}(\mathbf{W}^k, \mathbf{H}^k))$ and $\frac{1}{2}\lambda_{\max}(\nabla_{\mathbf{W}}^2 F_{\rho}(\mathbf{W}^k, \mathbf{H}^{k+1}))$, respectively. The stopping condition for Algorithm 2 and Algorithm 3 is the normalized residual of $(\mathbf{W}^k, \mathbf{H}^k)$ which is defined in the same way as (24) and is denoted as ϵ_{PALM} .

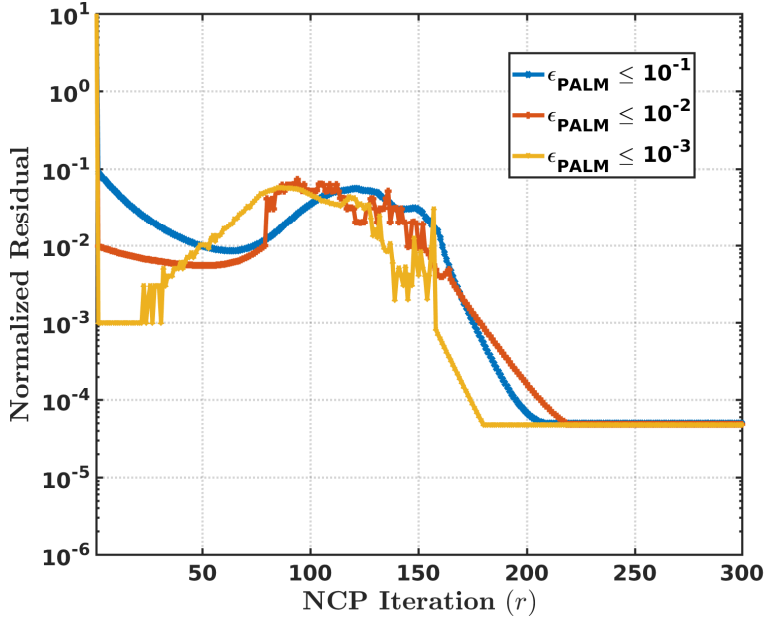
If not mentioned specifically, for the SNCP method, we set $\max\{\epsilon_{\text{orth}}, \epsilon_{\text{NR}}\} \leq 10^{-5}$ for Algorithm 1 and $\epsilon_{\text{PALM}} \leq 3 \times 10^{-3}$ for Algorithm 2; for the NSNCP method, we set $\max\{\epsilon_{\text{orth}}, \epsilon_{\text{NR}}\} \leq 10^{-3}$ for Algorithm 1 and $\epsilon_{\text{PALM}} \leq 3 \times 10^{-3}$ for Algorithm 3.

Algorithm convergence: Let us first examine the converge behavior of the proposed SNCP and NSNCP methods. Fig. 1(a) and Fig. 1(b) respectively display the normalized residual versus the iteration number of Algorithm 1 when the SNCP and NSNCP methods are used. The stopping condition of Algorithm 2 and Algorithm 3 are set to $\epsilon_{\text{PALM}} \leq 10^{-1}, 10^{-2}, 10^{-3}$, respectively. One can see from Fig. 1 that both SNCP and NSNCP methods converge, and the algorithm can converges faster for $\epsilon_{\text{PALM}} \leq 10^{-3}$. In Fig. 2, the orthogonality achieved by the SNCP and NSNCP methods are shown. One can observe that both methods indeed can achieve an orthogonal \mathbf{H} . Moreover, one can see that the NSNCP method takes about 150 iterations to reach $\epsilon_{\text{orth}} < 10^{-15}$, which is faster than the SNCP method.

SNCP vs NSNCP: To further examine the difference between the SNCP and NSNCP methods, we plot in Fig. 3 the clustering accuracy versus the stopping condition ϵ_{PALM} of Algorithm 2 and Algorithm 3, for the synthetic data with $\text{SNR} = -3$ dB. The results are averaged over 10 experiments, each of which uses a different initial point for Algorithm 1. The error bars (dashed line) are the standard deviation of the 10 experimental results. One can observe that the clustering accuracy improves with a smaller ϵ_{PALM} for both methods, though the SNCP method consistently outperforms the NSNCP method. However, the performance gap between the two methods reduces with smaller ϵ_{PALM} , and when $\epsilon_{\text{PALM}} \leq 3 \times 10^{-3}$, they yield comparable clustering performance.



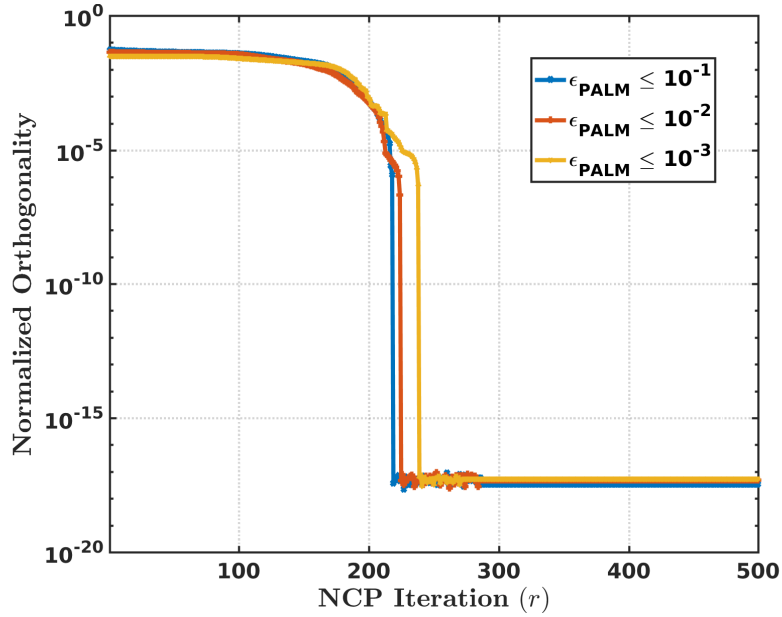
(a) SNCP



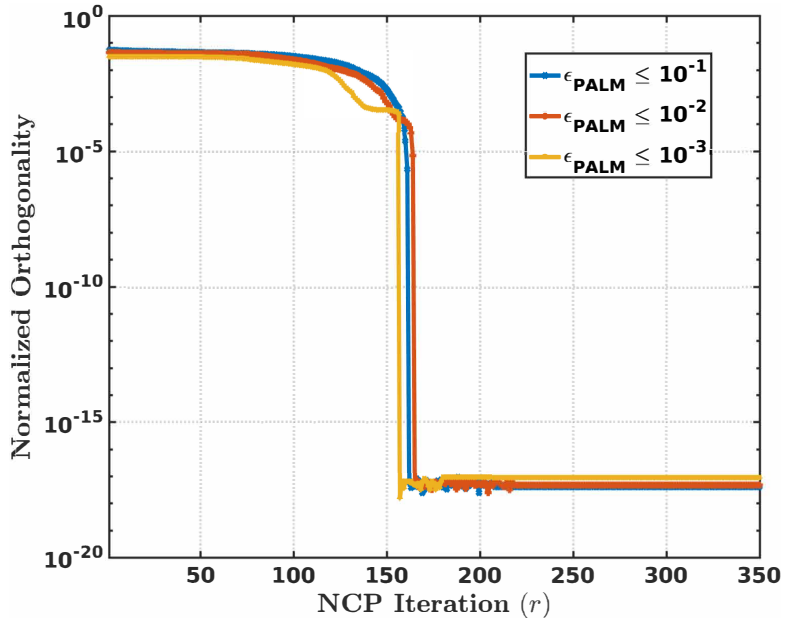
(b) NSNCP

Figure 1: Convergence curves of normalized residual achieved by the proposed (a) smooth NCP and (b) non-smooth NCP, for the synthetic data with $\text{SNR} = -1$ dB.

In Fig. 4(a), we further present the convergence curves of clustering accuracy versus the iteration number of Algorithm 1 for both the SNCP and NSNCP methods, on the synthetic data with $\text{SNR} = -3$ dB. Intriguingly, one can observe that the NSNCP method actually converges faster than the SNCP method, which echos Theorem 2 that the NSNCP method



(a) SNCP



(b) NSNCP

Figure 2: Convergence curves of orthogonality achieved by the proposed (a) smooth NCP and (b) non-smooth NCP, for the synthetic data with $\text{SNR} = -1$ dB.

requires a finite ρ only to achieve a feasible and meaningful solution of (8). However, as seen from the figure, the SNCP method eventually can reach a higher clustering accuracy than

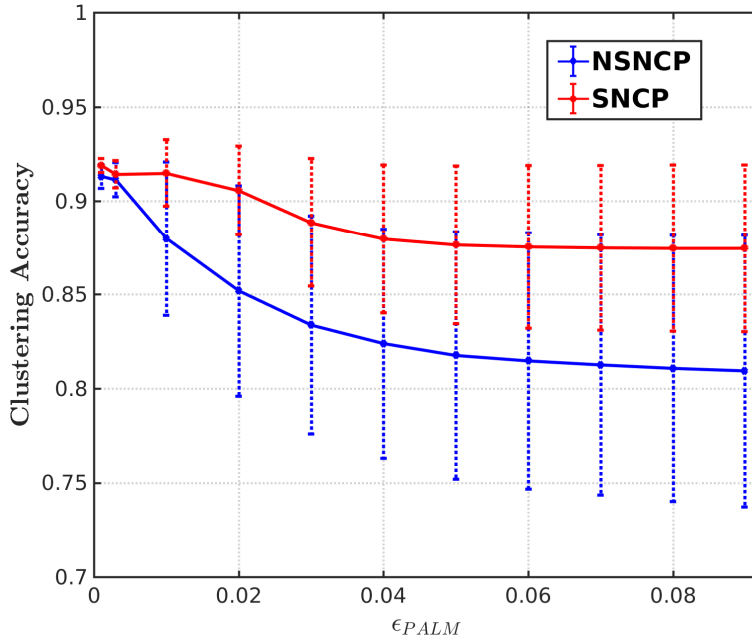


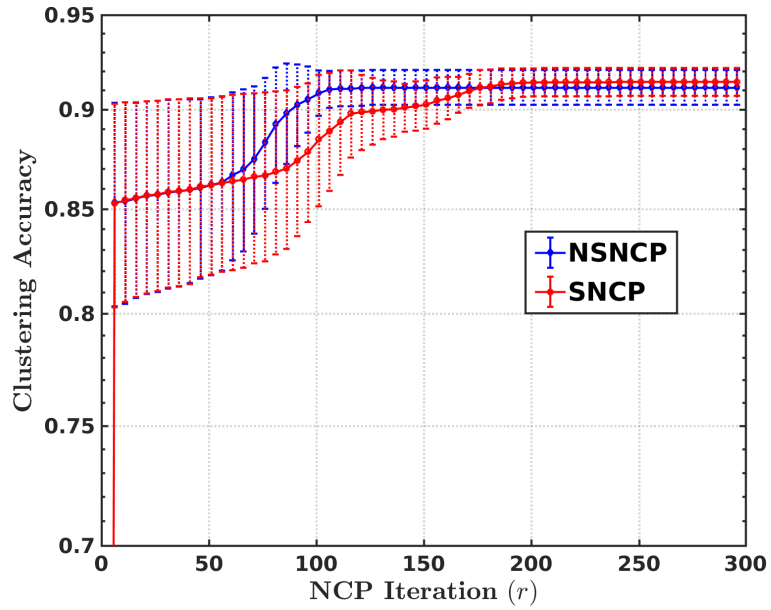
Figure 3: Comparison of the proposed SNCP and NSNCP methods in terms of clustering accuracy. Each point is averaged over 10 runs with different initials. And the error bar is the standard deviation of the 10 results.

the NSNCP method. Similar convergence behavior of the two methods are also observed for a document data set (dataset 1 in Table 2), as we show in Fig. 4(b).

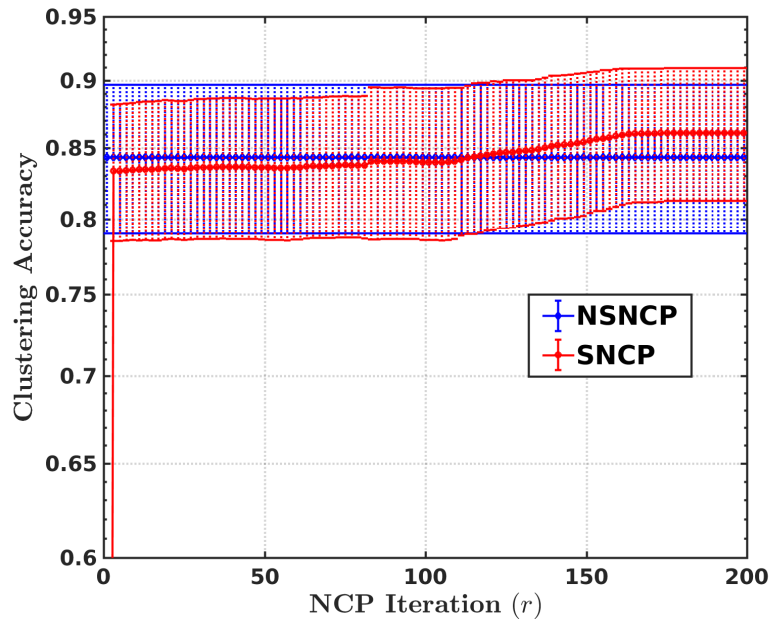
Clustering performance: Table 1 lists the average clustering performance (ARI and ACC) of the eight methods under test on the synthetic data with different SNR values. All results are obtained by averaging over 20 experiments. In each experiment, all methods use the same randomly generated initial point.

First of all, one can observe that K-means++ does not perform better than the K-means due to the presence of outliers. The ONMF based methods (i.e., DTPP, ONP-MF, ONMF-S, HALS, and proposed SNCP/NSNCP) significantly outperform the K-means and K-means++. Nevertheless, one can see from Table 1 that the proposed SNCP and NSNCP methods consistently yield the best clustering performance, especially for the clustering accuracy and when the SNR is low.

Computational time: Table 1 also shows the CPU time taken by each method. The computer used in the experiments have a Ubuntu 16.04 OS, 3.40 GHZ Intel Core i7-6700 CPU and 52 GB RAM. As seen, other than the K-Means and K-Means++ which are well known computationally cheap, the proposed SNCP and NSNCP methods are more computationally time efficient than the other five ONMF based methods. In particular, while the ONP-MF can provide competitive clustering performance when $SNR \geq 1$ dB, its computation time is large. By contrast, the HALS can provide reasonably good clustering performance when $SNR \geq 1$ dB and its computation time is moderate. Lastly, we note that the NSNCP method is slightly faster than the SNCP method, though the latter can provide the best clustering performance.



(a)



(b)

Figure 4: Clustering accuracy versus of NCP iteration of the proposed SNCP and NSNCP methods, for (a) the synthetic data with $\text{SNR} = -3$ dB, and (b) the document data set 1 (Table 2).

Table 1: Average clustering performance (%) and CPU time (s) on the synthetic data for different values of SNR.

SNR (dB)		-5	-3	-1	1	3	5
ARI	KM	57.0	65.8	73.8	73.6	73.4	68.7
	KM++	57.1	66.9	63.7	66.8	65.3	72.9
	DTPP	78.5	82.8	83.0	84.4	83.5	86.9
	ONP-MF	56.6	87.0	80.2	89.6	89.6	89.2
	ONMF-S	71.2	73.4	75.7	76.3	76.8	77.1
	HALS	67.9	81.9	85.2	87.2	87.0	86.2
	SNCP	91.1	91.1	91.3	91.5	91.8	91.9
NSNCP	89.8	90.3	91.1	91.2	91.5	91.7	
ACC	KM	63.4	69.7	74.7	74.3	75.6	73.7
	KM++	64.1	70.1	70.3	70.8	69.2	75.5
	DTPP	81.6	85.1	85.9	87.0	86.6	89.4
	ONP-MF	66.8	88.3	83.1	89.9	90.0	90.4
	ONMF-S	77.4	79.0	80.2	81.3	81.7	81.9
	HALS	76.3	86.0	88.1	89.6	89.4	89.3
	SNCP	91.5	91.6	91.8	92.4	92.9	93.3
NSNCP	90.3	90.8	91.7	91.8	92.6	92.8	
Time	KM	3.10	1.96	1.52	1.16	1.11	1.01
	KM++	3.09	2.44	2.05	1.70	1.59	1.59
	DTPP	30.4	34.0	38.6	31.1	35.1	30.7
	ONP-MF	1097	1123	1124	1153	1148	1129
	ONMF-S	68.4	97.1	116	116	90.5	104.6
	HALS	22.6	25.6	23.3	15.7	19.3	16.7
	SNCP	18.2	12.6	11.4	10.1	9.23	9.34
NSNCP	14.3	10.6	9.06	8.70	8.57	8.50	

Clustering stability: We evaluate the stability of the clustering methods against different initial points. In particular, we adopt the consensus map and cophenetic correlation (CC) coefficient (Brunet et al., 2004) to measure the stability. Roughly speaking, in the consensus map, the (i, j) th entry will be close to 1 if sample i and sample j are consistently assigned to the same cluster even under different initial conditions. The CC coefficient (between 0 and 1) is used to quantize the overall quality of the consensus map. Fig. 5 shows the results for SNR = -3 dB, and one can see that the proposed SNCP method gives the stablest clustering results, which is followed by the NSNCP method. In particular, inconsistency only happens in small-sized clusters for these two methods.

Robustness to parameter K : Most of the clustering methods require one to specify the cluster number K in advance. Here we test the robustness of the proposed methods by deliberately setting $K = 20$, which is twice larger than the cluster number of the ground truth data. Fig. 6 displays the average size of each cluster obtained by the proposed SNCP method, HALS, and K-means, on the synthetic data with SNR = -3 dB. The clusters are ordered in the descending order of their size, and ‘‘Ground truth’’ is the true cluster distribution of the synthetic data. As seen, the proposed SNCP method yields the most consistent result with the ground truth, and only a few samples are assigned to cluster with index greater than 10. It is found that although the K-means also captures the true 10 clusters, it mistakenly breaks the biggest cluster and assigns many of the samples to 2nd largest cluster. Moreover, one can also observe that the HALS method does not perform

well as its cluster sizes are very different from the ground truth for cluster indices larger than 6, and quite some samples are assigned to cluster index larger than 10.

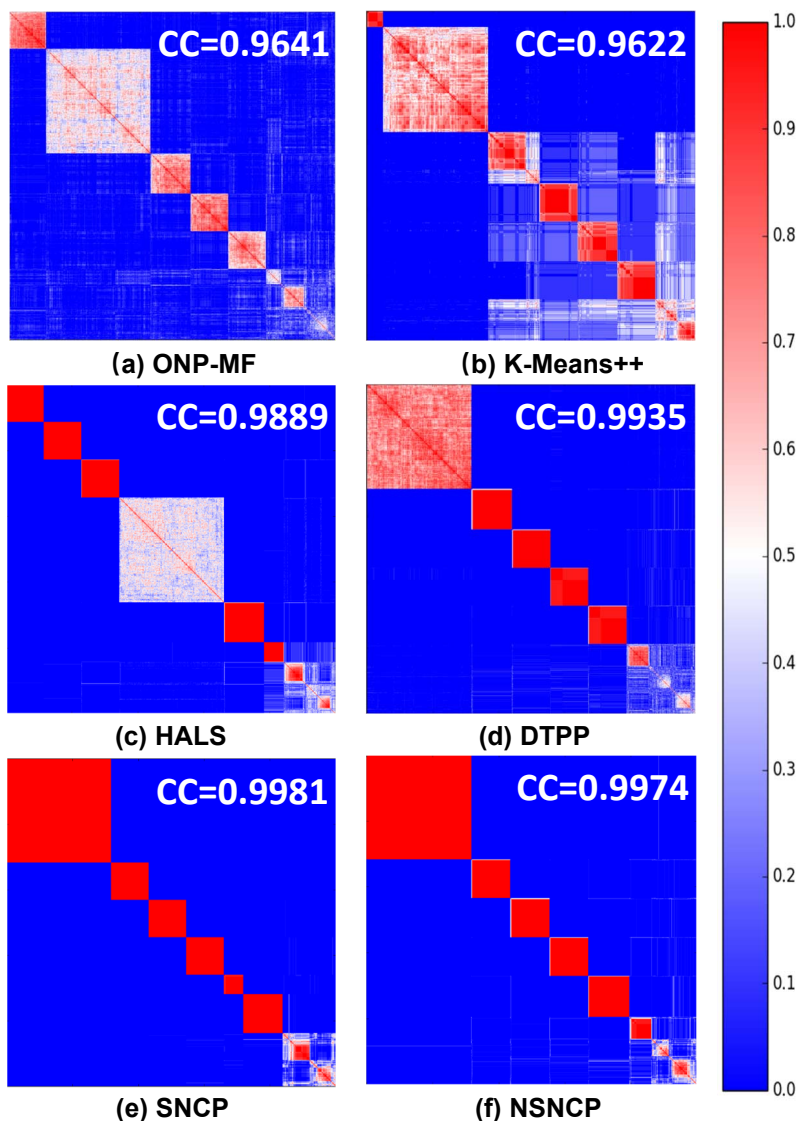


Figure 5: The consensus map of clustering results for the synthetic data with SNR = -5 dB.

5.2 Application to Document Clustering

We examine the performance of the proposed methods on the real dataset TDT2 corpus (Cai et al., 2011) which consists of 10212 on-topic documents in total with 56 semantic categories. We extract 7 subsets, each of which contains 10 randomly picked categories ($K = 10$). Each document sample is normalized and represented as a term-frequency-inverse-document-frequency (tf-idf) vector (Cai et al., 2011). The dimension of each test

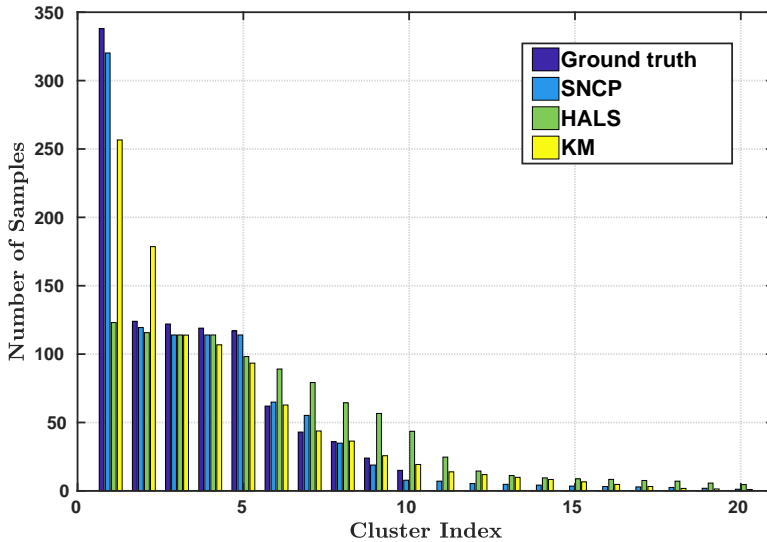


Figure 6: The average size of each cluster obtained by SNCP, HALS and KM with $K = 20$.

data is shown in the first three rows of Table 2. In the experiment, we set $\nu = 10^{-8}$ and $\mu = 0$ for the proposed SNCP, and $\nu = \mu = 0$ for the NSNCP method. For the NSNCP method, it is set that $\epsilon_{\text{orth}} \leq 10^{-5}$ and $t^k = \frac{1}{2} \|\nabla_{\mathbf{H}}^2 \tilde{F}(\mathbf{W}^k, \mathbf{H}^k)\|_F$ for Algorithm 3.

Performance comparison: As seen from Table 2, for this TDT2 data, the ONMF based methods do not have significant performance advantage over the K-means/K-means++. In particular, K-means++ yields the highest ARI and clustering accuracy on Dataset 5, and K-means gives comparable performance on Dataset 6 and Dataset 7. A close inspection shows that for Dataset 5, the initial points picked by K-means++ happens to be close to the cluster centroids of the ground truth.

We can see that, except for Dataset 3 and 5, the proposed SNCP method performs best. It is also noted that except for Dataset 2, the ONMF-S and ONP-MF can provide either close or slightly better performance than the proposed SNCP method. However, as seen from Table 2, the computation time of the two methods are large and can be 50 times slower than the proposed SNCP method on Dataset 6 and 7. It is also seen that the HALS is most time efficient on this experiment although it only provides moderate clustering performance. While the NSNCP method does not perform as well as its smooth counterpart, it gives comparable clustering performance for the first four dataset, and is computationally time efficient compared to ONMF-S and ONP-MF.

Clustering on dimension-reduced data: In view of the fact that dimension reduction techniques can extract low-rank structure of data and improve the clustering performance, we apply the spectral clustering (SC) (Luxburg, 2007) to the TDT2 data followed by applying the various clustering methods to the dimension-reduced data. In the experiment, we set $\nu = \mu = 0$ and each entry of \mathbf{W} is lower (resp. upper) bounded by the minimum (resp. maximum) value of the dimension-reduced data. The experimental results are displayed in Table 3. As observed, all methods have a great leap in the clustering performance when compared to Table 2, and there is no significant performance gap between various methods. Nevertheless, the proposed SNCP method can provide competitive clustering results and

Table 2: Average clustering performance (%) and CPU time (s) on TDT2 data.

Dataset		1	2	3	4	5	6	7
#terms M		13133	24968	11079	20431	16067	29725	26577
#docs N		842	3292	631	1745	1079	4779	4264
ARI	KM	66.7	35.3	82.6	34.4	55.9	56.2	39.1
	KM++	71.0	35.8	82.9	32.2	55.1	53.2	39.5
	DTPP	72.0	33.0	81.0	45.8	36.7	54.7	38.0
	ONMF-S	78.8	33.8	84.7	50.3	41.1	56.0	36.4
	ONP-MF	78.8	28.0	86.1	46.1	48.4	52.0	38.5
	HALS	78.1	32.1	87.0	45.4	39.9	52.5	37.0
	SNCP	88.3	36.4	87.1	51.5	48.9	60.7	40.2
NSNCP	87.9	35.8	88.2	50.5	44.8	52.7	37.1	
ACC	KM	77.9	51.7	84.4	49.3	61.3	70.2	49.8
	KM++	73.5	48.9	84.7	47.1	61.7	65.7	50.2
	DTPP	70.0	50.4	77.4	52.1	45.1	66.6	47.8
	ONMF-S	81.8	52.0	83.6	59.6	50.9	68.8	48.0
	ONP-MF	85.3	46.1	89.5	60.9	59.4	66.8	50.4
	HALS	77.9	47.8	85.1	54.3	48.7	64.4	48.0
	SNCP	86.1	56.8	88.1	62.0	58.2	70.7	52.5
NSNCP	84.3	54.2	87.8	60.4	54.7	66.6	47.5	
Time	KM	13.6	195	6.82	65.0	27.4	318	283
	KM++	10.6	199	8.15	53.6	28.9	401	317
	DTPP	126	726	81	413	204	2282	1560
	ONMF-S	405	8124	157	1915	633	17603	12041
	ONP-MF	1200	7854	757	3660	1951	14302	11626
	HALS	12.9	35.6	6.07	27.4	20.0	162	97.9
	SNCP	37.3	407	20.4	64.0	41.1	263	238
NSNCP	24.5	378	14.6	60.8	40.3	281	146	

performs best on Dataset 1, 2, and 6. Although the ONP-MF performs best on Dataset 3 and 5, it remains to be expensive in computation time. While the K-means++ gives the best performance on Dataset 4 and 7, one can see that the proposed SNCP method is only slighter worse.

5.3 Application to Image Analysis

In the last example, we apply the various clustering methods to the MNIST dataset which contains both training and testing image samples of handwritten digits from 0 to 9 (LeCun et al.). Each image sample is a 784×1 vector ($M = 784$). We consider 7 subsets with different numbers of sample size (N) as shown in the 2nd row of Table 4. In particular, Dataset 1, 2, 3, and 4 are constituted by randomly picking 200, 400, 600, and 800 training samples of each of the 10 digits, respectively. Dataset 5 consists of clusters with unequal sizes, that is, 200 training samples for digits 0 to 3, 400 training samples for digits 4 to 6, 600 training samples for digits 7 and 8, and 800 training samples for digit 9. Dataset 6 contains all the 10000 test samples for the 10 digits. Dataset 7 contains the first 2000 training samples and the first 2000 test samples of all 10 digits. It is set that $\nu = 10^{-10}$ and $\mu = 0$, and each entry of \mathbf{W} is upper bounded by the maximum value of the datasets, for the proposed SNCP method. The other parameters are set the same as that in Section 5.1.

Performance comparison: One can see from Table 4 that the proposed SNCP method performs best, especially for the first five dataset. Comparing to the proposed SNCP

Table 3: Average clustering performance (%) and CPU time (s) on dimension-reduced TDT2 data

Dataset		1	2	3	4	5	6	7
Time of SC		13.8	402	7.11	90.7	30.7	1114	839
ARI	SC+KM	77.7	58.8	78.8	81.7	88.2	72.1	60.9
	SC+KM++	96.7	77.8	97.9	99.3	98.0	82.7	72.3
	SC+HALS	93.3	78.3	96.6	97.7	99.1	80.2	69.0
	SC+ONP-MF	97.6	77.9	98.4	98.9	99.3	79.9	69.8
	SC+SNCP	98.0	79.3	97.6	98.8	99.4	83.4	71.3
ACC	SC+KM	81.6	69.0	83.1	86.3	89.1	80.2	69.8
	SC+KM++	98.3	83.3	98.9	99.6	98.9	90.3	82.6
	SC+HALS	95.8	82.8	97.8	98.8	99.4	90.8	78.7
	SC+ONP-MF	98.6	82.3	99.0	99.3	99.5	89.7	80.9
	SC+SNCP	99.0	84.3	98.0	99.2	99.3	92.7	81.4
Time	SC+KM	0.24	1.34	0.17	0.45	0.33	2.33	1.28
	SC+KM++	0.25	1.96	0.18	0.46	0.34	2.18	2.06
	SC+HALS	0.78	2.45	0.81	1.65	0.75	1.52	2.03
	SC+ONP-MF	13.6	385	7.29	90.0	26.0	790	626
	SC+SNCP	0.59	2.00	0.55	1.31	1.21	3.17	2.86

Table 4: Average clustering performance (%) and CPU time (s) on the MNIST data.

Dataset		1	2	3	4	5	6	7
#images N		2000	4000	6000	8000	4000	10000	4000
ARI	KM	36.0	37.6	36.8	36.9	27.8	37.2	31.4
	KM++	36.3	38.0	37.1	36.6	27.6	39.1	31.9
	DTPP	34.4	36.2	36.6	36.7	26.7	35.0	32.5
	ONMF-S	32.5	30.7	32.8	34.9	27.9	33.3	31.1
	ONP-MF	29.5	27.9	28.5	30.8	21.6	31.2	24.6
	HALS	31.3	33.0	33.7	33.9	28.6	34.0	31.8
	SNCP	41.2	40.2	39.8	39.3	30.3	37.0	35.2
ACC	KM	54.3	55.2	54.4	54.5	46.5	53.2	49.4
	KM++	54.1	56.0	55.1	53.9	45.5	55.5	50.8
	DTPP	54.2	56.1	57.1	57.0	44.6	55.4	54.1
	ONMF-S	49.4	48.1	50.3	52.5	45.2	51.4	50.8
	ONP-MF	46.5	45.5	46.2	47.9	40.2	46.7	43.2
	HALS	50.5	53.7	54.0	54.1	45.8	55.6	54.1
	SNCP	61.1	59.7	58.3	57.9	49.1	55.8	54.8
Time	KM	3.52	7.96	12.1	22.3	9.58	22.0	9.98
	KM++	3.45	8.24	13.0	21.4	10.7	26.1	12.0
	DTPP	55.2	185	382	795	188	897	182
	ONMF-S	92.7	251	561	918	222	1367	250
	ONP-MF	825	2818	5262	10654	3062	14834	2935
	HALS	8.02	7.61	12.4	13.7	8.54	18.6	8.57
	SNCP	23.6	44.6	67.0	74.3	34.5	84.9	33.6

method, the ONMF-S and ONP-MF are not as competitive as in Table 2. Interestingly, it is observed that the DTPP, which does not perform well in Table 1 and Table 2, performs comparably on this MNIST dataset, and outperforms the ONMF-S and ONP-MF. Besides, the HALS exhibits comparable clustering performance as the proposed SNCP method, especially on Dataset 6 and 7, though there still exist considerable performance gap between the two methods in the first five dataset.

6. Conclusion

In this paper, we have proposed the ONMF based data clustering formulation (8) and the NCP approach (14) and Algorithm 1. We have considered one smooth NCP formulation (15) and one non-smooth NCP formulation (20), and analyzed the theoretical conditions of the two methods for which a feasible and stationary solution of (8) can be obtained. Efficient implementations of the proposed methods based on the PALM algorithm (Algorithm 2 and Algorithm 3) are also presented. Extensive experiments have been conducted based on the synthetic data and real data TDT2 and MNIST. In particular, when comparing to the existing K-means and ONMF based methods, the proposed methods can perform either significantly better or comparably in terms of ARI and clustering accuracy, while being much more time efficient than most of the other ONMF based methods. The performance improvement of the proposed method is partially attributed to its stability with respect to the initial point for optimization, in contrast to the K-means (see Fig. 5).

It is worthwhile to mention some interesting directions for future research. Firstly, while the current PLAM algorithms seem to work well, it is possible to employ some more advanced optimization algorithms such as Nesterov’s accelerated method (Lin et al., 2014; Phan et al., 2018; Fercoq and Richtarik, 2015) to improve algorithm convergence speed. Secondly, while parallel and distributed implementations of the proposed methods are feasible, it is important to reduce the communication overhead between cluster nodes for large-scale scenarios (Balcan et al., 2013; Bhaskara and Wijewardena, 2018). It is also interesting to study joint dimension reduction and clustering methods (Yang et al., 2017a) using the proposed NCP methods, and extend the current Euclidean distance measure to more general cost functions such as the β -divergence (Fevotte and Idier, 2011; Liu et al., 2012) or the cohesion measure proposed in (Chang et al., 2016).

Acknowledgments

We would like to acknowledge support for this project from the National Science Foundation of China (NSFC) under Grant 61571385 and 61731018, and the Shenzhen Fundamental Research Fund under Grant ZDSYS201707251409055 and KQTD2015033114415450.

Appendix A. Proof of Proposition 2

Proof of (a): Denote $\mathbf{Z}^* \triangleq (\mathbf{W}^*, \mathbf{H}^*)$, and \mathcal{Z} as the feasible set in (15b). Moreover, let $\mathcal{N}_\epsilon(\mathbf{Z}^*) = \{\mathbf{Z} \mid \|\mathbf{Z} - \mathbf{Z}^*\|_F^2 \leq \epsilon\}$, where $\epsilon > 0$, be a neighborhood of \mathbf{Z}^* such that $G_\rho(\mathbf{Z}^*) \leq G_\rho(\mathbf{Z})$ for all $\mathbf{Z} \in \mathcal{N}_\epsilon(\mathbf{Z}^*) \cap \mathcal{Z}$.

Let $\phi(\mathbf{h}_j) = (\mathbf{1}^T \mathbf{h}_j)^2 - \|\mathbf{h}_j\|_2^2$. Note that, as long as $\phi(\mathbf{h}_j) > 0$ (i.e., if \mathbf{h}_j has at least two nonzero entries), $\phi(\mathbf{h}_j)$ is an increasing function with respect to every entry of \mathbf{h}_j . Suppose that there exists an index $j' \in \mathcal{N}$ such that $\mathbf{h}_{j'}^*$ is infeasible to (8c) and thus $\phi(\mathbf{h}_{j'}^*) > 0$. Then, for a scalar $\alpha \in (0, 1)$ that is sufficiently close to one, $\mathbf{Z}_\alpha \triangleq (\frac{1}{\alpha} \mathbf{W}^*, \alpha \mathbf{H}^*)$ is a feasible point to (15) and it achieves a smaller objective value than \mathbf{Z}^* , i.e., $G_\rho(\mathbf{Z}_\alpha) < G_\rho(\mathbf{Z}^*)$.

Specifically, since

$$\begin{aligned}\|\mathbf{Z}_\alpha - \mathbf{Z}^*\|^2 &= \left(\frac{1}{\alpha} - 1\right)^2 \|\mathbf{W}^*\|_F^2 + (\alpha - 1)^2 \|\mathbf{H}^*\|_F^2 \\ &\leq \max\left\{\left(\frac{1}{\alpha} - 1\right)^2, (\alpha - 1)^2\right\} \|\mathbf{Z}^*\|_F^2,\end{aligned}\quad (25)$$

to have $\mathbf{Z}_\alpha \in \mathcal{N}_\epsilon(\mathbf{Z}^*)$, it is sufficient to let

$$\max\left\{1 - \beta, \frac{1}{1 + \beta}\right\} < \alpha < 1, \quad (26)$$

where $\beta = \sqrt{\frac{\epsilon}{2\|\mathbf{Z}^*\|_F^2}}$. Thus, we obtain a contradiction and \mathbf{H}^* must satisfy (8c) and is a local minimizer of (8) for $\mu = 0$.

Proof of (b): As $(\mathbf{W}^*, \mathbf{H}^*)$ is a local minimizer of problem (15), there exists a neighborhood of \mathbf{H}^* , denoted by $\mathcal{N}_\epsilon(\mathbf{H}^*) = \{\mathbf{H} \in \mathcal{H}^+ \mid \|\mathbf{H} - \mathbf{H}^*\|_F^2 \leq \epsilon\}$, such that

$$G_\rho(\mathbf{W}^*, \mathbf{H}^*) \leq G_\rho(\mathbf{W}^*, \mathbf{H}), \forall \mathbf{H} \in \mathcal{N}_\epsilon(\mathbf{H}^*). \quad (27)$$

Suppose there exists a j' such that $\mathbf{1}^T \mathbf{h}_{j'}^* \neq \|\mathbf{h}_{j'}^*\|_2$. Let $c \triangleq \mathbf{1}^T \mathbf{h}_{j'}^*$,

$$\Phi \triangleq \{\ell \in \mathcal{K} \mid [\mathbf{H}^*]_{\ell, j'} > 0\} = \{i_1, i_2, \dots, i_{|\Phi|}\},$$

and define a hyperplane $\mathcal{H}_c \triangleq \{\mathbf{H} \in \mathcal{H}^+ \mid \mathbf{1}^T \mathbf{h}_{j'} = c\}$. We will show a contradiction that there exists a neighbor of \mathbf{H}^* that lies in the hyperplane \mathcal{H}_c and achieves a smaller objective than \mathbf{H}^* .

To the end, for $\ell = 1, \dots, |\Phi|$, let

$$\mathbf{H}^{(\ell)} = \sum_{j \neq j'} \mathbf{h}_j^* \mathbf{e}_j^T + \mathbf{h}_{j'}^{(\ell)} \mathbf{e}_{j'}^T, \quad (28)$$

which is obtained by replacing the j' th column of \mathbf{H}^* by

$$\mathbf{h}_{j'}^{(\ell)} \triangleq \alpha_\ell \mathbf{s}^{(\ell)} + (1 - \alpha_\ell) \mathbf{h}_{j'}^*, \quad (29)$$

where $0 < \alpha_\ell < 1$ and $\mathbf{s}^{(\ell)} \triangleq c \mathbf{e}_{i_\ell}$. One can see that $\mathbf{H}^{(\ell)} \in \mathcal{H}_c$ since

$$\mathbf{1}^T \mathbf{h}_{j'}^{(\ell)} = \alpha_\ell c + (1 - \alpha_\ell) c = c. \quad (30)$$

Firstly, we show that \mathbf{H}^* is a convex combination of $\mathbf{H}^{(\ell)}, \forall \ell = 1, \dots, |\Phi|$. By (29), we have $\mathbf{s}^{(\ell)} = \frac{\mathbf{h}_{j'}^{(\ell)} - (1 - \alpha_\ell) \mathbf{h}_{j'}^*}{\alpha_\ell}$. Thus, we can obtain

$$\mathbf{h}_{j'}^* = \sum_{\ell=1}^{|\Phi|} [\mathbf{H}^*]_{i_\ell, j'} \mathbf{e}_{i_\ell} = \sum_{\ell=1}^{|\Phi|} \beta^\ell \left(\frac{\mathbf{h}_{j'}^{(\ell)} - (1 - \alpha_\ell) \mathbf{h}_{j'}^*}{\alpha_\ell} \right), \quad (31)$$

where $\beta_\ell \triangleq \frac{[\mathbf{H}^*]_{i_\ell, j'}}{c}$. Rearranging the terms in (31) gives rise to

$$\left(1 + \sum_{\ell=1}^{|\Phi|} \frac{\beta_\ell}{\alpha_\ell} (1 - \alpha_\ell)\right) \mathbf{h}_{j'}^* = \sum_{\ell=1}^{|\Phi|} \frac{\beta_\ell}{\alpha_\ell} \mathbf{h}_{j'}^{(\ell)}. \quad (32)$$

Notice that $\sum_{\ell=1}^{|\Phi|} \beta_\ell = \sum_{\ell=1}^{|\Phi|} \frac{[\mathbf{H}^*]_{i_\ell, j'}}{c} = \frac{\mathbf{1}^T \mathbf{h}_{j'}^*}{c} = 1$. So (32) reduces to

$$\mathbf{h}_{j'}^* = \sum_{\ell=1}^{|\Phi|} \frac{\beta_\ell}{\alpha_\ell} \mathbf{h}_{j'}^{(\ell)} \Big/ \sum_{\ell=1}^{|\Phi|} \frac{\beta_\ell}{\alpha_\ell} \triangleq \sum_{\ell=1}^{|\Phi|} \gamma_\ell \mathbf{h}_{j'}^{(\ell)}, \quad (33)$$

which implies that \mathbf{H}^* is a convex combination of $\mathbf{H}^{(\ell)}$, $\ell = 1, \dots, |\Phi|$.

Secondly, we show that $G_\rho(\mathbf{W}^*, \mathbf{H})$ is strongly concave with respect to \mathbf{H} on the hyperplane \mathcal{H}_c as long as ρ is sufficiently large. It is sufficient to show that $G_\rho(\mathbf{W}^*, \mathbf{H}) - \frac{\rho}{2} \sum_{j=1}^N \mathbf{1}^T \mathbf{h}_j = F(\mathbf{W}^*, \mathbf{H}) - \frac{\rho}{2} \sum_{j=1}^N \|\mathbf{h}_j\|_2^2$ is strongly concave in \mathbf{H} . This is true since $\nabla_{\mathbf{H}} F(\mathbf{W}, \mathbf{H})$ is Lipschitz continuous with a bounded Lipschitz constant (denoted by ρ^*), and thus $F(\mathbf{W}^*, \mathbf{H}) - \frac{\rho}{2} \sum_{j=1}^N \|\mathbf{h}_j\|_2^2$ will be a strongly concave function as long as $\rho > \rho^*$.

By the above two facts, we obtain that

$$G_\rho(\mathbf{W}^*, \mathbf{H}^*) > \sum_{\ell=1}^{|\Phi|} \gamma_\ell G_\rho(\mathbf{W}^*, \mathbf{H}^{(\ell)}) \geq G_\rho(\mathbf{W}^*, \mathbf{H}^{(\ell')}), \quad (34)$$

where $\ell' = \arg \min_{\ell=1, \dots, |\Phi|} G_\rho(\mathbf{W}^*, \mathbf{H}^{(\ell)})$. Since by (29), $\mathbf{H}^{(\ell')}$ will lie in $\mathcal{N}_\epsilon(\mathbf{H}^*)$ for $\alpha_{\ell'} < \frac{\epsilon}{c - [\mathbf{H}^*]_{i_{\ell'}, j'}}$, (34) shows a contradiction to the local optimality of \mathbf{H}^* . Thus, for $\rho > \rho^*$, \mathbf{H}^* must be feasible and a local minimizer to (8). \blacksquare

Appendix B. Proof of Theorem 1

Proof of (a): Let $\phi(\mathbf{h}_j) \triangleq (\mathbf{1}^T \mathbf{h}_j)^2 - \|\mathbf{h}_j\|_2^2$. Since $(\mathbf{W}^\rho, \mathbf{H}^\rho)$ is a stationary point of (14), we have

$$\langle \nabla_{\mathbf{H}} F(\mathbf{W}^\rho, \mathbf{H}^\rho), \mathbf{D} \rangle + \frac{\rho}{2} \sum_{j=1}^N \langle \nabla \phi(\mathbf{h}_j^\rho), \mathbf{d}_j \rangle \geq 0, \forall \mathbf{D} \in \mathcal{T}_{\mathcal{H}^+}(\mathbf{H}^\rho), \quad (35)$$

where

$$\mathcal{T}_{\mathcal{H}^+}(\mathbf{H}^\rho) = \{\mathbf{D} \in \mathbb{R}^{K \times N} \mid [\mathbf{D}]_{ij} \geq 0 \text{ if } [\mathbf{H}^\rho]_{ij} = 0, \forall i \in \mathcal{K}, j \in \mathcal{N}\}. \quad (36)$$

Suppose that \mathbf{H}^∞ does not satisfy (8c). Specifically, there exists an index $j' \in \mathcal{N}$ such that $\phi(\mathbf{h}_{j'}^\infty) > 0$, and suppose that the second largest entry in $\mathbf{h}_{j'}^\infty$, denoted by $[\mathbf{H}^\infty]_{i'j'}$, has a value no less than $\Delta > 0$.

Thus, for ρ is sufficiently large, $\phi(\mathbf{h}_{j'}^\rho) > 0$ and $[\mathbf{H}^\rho]_{i'j'} \geq \Delta$. Let us choose a tangent $\mathbf{D}^\rho \in \mathcal{T}_{\mathcal{H}}(\mathbf{H}^\rho)$ such that $[\mathbf{D}^\rho]_{i'j'} = -1$ and $[\mathbf{D}^\rho]_{ij} = 0$ otherwise. By substituting \mathbf{D}^ρ into (35)

$$\begin{aligned} 0 &\leq -[\nabla_{\mathbf{H}} F(\mathbf{W}^\rho, \mathbf{H}^\rho)]_{i', j'} - \rho(\mathbf{1}^T \mathbf{h}_{j'}^\rho - [\mathbf{H}^\rho]_{i'j'}) \\ &< -[\nabla_{\mathbf{H}} F(\mathbf{W}^\rho, \mathbf{H}^\rho)]_{i', j'} - \rho\Delta. \end{aligned} \quad (37)$$

Since $\nabla_{\mathbf{H}}F(\mathbf{W}^\rho, \mathbf{H}^\rho)$ is bounded due to bounded (\mathbf{W}, \mathbf{H}) , (37) cannot hold true when $\rho \rightarrow \infty$. Thus, \mathbf{H}^∞ must be feasible to (8).

Proof of (b): Theorem 1(b) can be obtained by applying Proposition 3 below to (8) and (15):

Proposition 3 *Consider the following problem*

$$\min_{\mathbf{x} \in \mathbb{R}^n} f(\mathbf{x}) \quad (38a)$$

$$\text{s.t.} \quad \left. \begin{array}{l} h_j(\mathbf{x}) = 0, \quad j \in \mathcal{N}, \\ g_i(\mathbf{x}) \leq 0, \quad i \in \mathcal{K}, \end{array} \right\} \triangleq \mathcal{X}, \quad (38b)$$

where f , h_j and g_i are all smooth, g_i are convex but f and h_j are not necessarily convex. Assume that $h_j(\mathbf{x}) \geq 0$ for all $\mathbf{x} \in \text{dom}(h_j)$, and consider the following penalized formulation

$$\min_{\mathbf{x} \in \mathbb{R}^n} f(\mathbf{x}) + \rho \sum_{j=1}^N h_j(\mathbf{x}) \quad (39a)$$

$$\text{s.t.} \quad g_i(\mathbf{x}) \leq 0, \quad i \in \mathcal{K} \quad (39b)$$

where $\rho > 0$ is a penalty parameter. Let \mathbf{x}^ρ be a stationary point of (39). Assume that $\mathbf{x}^\rho \rightarrow \mathbf{x}^\infty$ as $\rho \rightarrow \infty$, and

(A1) \mathbf{x}^∞ is feasible to problem (38),

(A2) The MFCQ holds for problem (38) at \mathbf{x}^∞ , i.e., $\nabla h_j(\mathbf{x}^\infty)$, $j = 1, \dots, N$, are linearly independent, and there exists a vector $\mathbf{d}^\infty \in \mathbb{R}^n$ such that

$$\langle \nabla h_j(\mathbf{x}^\infty), \mathbf{d}^\infty \rangle = 0, \quad \forall j \in \mathcal{N}, \quad (40)$$

$$\langle \nabla g_i(\mathbf{x}^\infty), \mathbf{d}^\infty \rangle < 0, \quad \forall i \in \mathcal{I}^\infty, \quad (41)$$

where $\mathcal{I}^\infty = \{i \in \mathcal{K} \mid g_i(\mathbf{x}^\infty) = 0\}$. Then, \mathbf{x}^∞ is a B-stationary point of (38).

The proof is given in Appendix C. Proposition 3 can be regarded as an extension of the smooth penalty method in (Nocedal and Wright, 2006, Theorem 17.2) to the partial smooth penalty in (39). \blacksquare

Appendix C. Proof of Proposition 3

Since \mathbf{x}^ρ be a stationary point of (39) and $\{g_i(\mathbf{x})\}$ are smooth convex, it satisfies

$$\langle \nabla f(\mathbf{x}^\rho), \mathbf{d} \rangle + \rho \sum_{j=1}^N \langle \nabla h_j(\mathbf{x}^\rho), \mathbf{d} \rangle \geq 0, \quad \forall \mathbf{d} \in \{\mathbf{d} \in \mathbb{R}^n \mid \langle \nabla g_i(\mathbf{x}^\rho), \mathbf{d} \rangle \leq 0, \quad i \in \mathcal{I}^\rho\}, \quad (42)$$

where $\mathcal{I}^\rho = \{i \in \mathcal{K} \mid g_i(\mathbf{x}^\rho) = 0\}$. Since the MFCQ holds at \mathbf{x}^∞ , MFCQ also holds at \mathbf{x}^ρ for sufficiently large ρ (Facchinei and Pang, 2003, page 255); in particular, $\nabla h_j(\mathbf{x}^\rho)$, $j = 1, \dots, N$, are linearly independent, and there exists a vector $\mathbf{d}^\rho \in \mathbb{R}^n$ such that

$$\langle \nabla h_j(\mathbf{x}^\rho), \mathbf{d}^\rho \rangle = 0, \quad \forall j \in \mathcal{N}, \quad (43)$$

$$\langle \nabla g_i(\mathbf{x}^\rho), \mathbf{d}^\rho \rangle < 0, \quad \forall i \in \mathcal{I}^\infty. \quad (44)$$

Therefore, when ρ is sufficiently large, it is feasible to have from (42) that

$$\begin{aligned} \langle \nabla f(\mathbf{x}^\rho), \mathbf{d} \rangle &\geq 0, \\ \forall \mathbf{d} \in \left\{ \mathbf{d} \in \mathbb{R}^n \mid \begin{array}{l} \langle \nabla h_j(\mathbf{x}^\rho), \mathbf{d} \rangle = 0, \quad \forall j = 1, \dots, N, \\ \langle \nabla g_i(\mathbf{x}^\rho), \mathbf{d} \rangle \leq 0, \quad i \in \mathcal{I}^\infty \end{array} \right\}. \end{aligned} \quad (45)$$

By (45) and by the Farkas lemma (Nocedal and Wright, 2006, Theorem 12.4), there exist variables $\boldsymbol{\lambda}^\rho = \{\lambda_j^\rho\}_{j=1}^N$ and $\boldsymbol{\nu}^\rho = \{\nu_i^\rho\}_{i \in \mathcal{I}^\infty}$ such that

$$\nabla f(\mathbf{x}^\rho) + \sum_{j=1}^N \lambda_j^\rho \nabla h_j(\mathbf{x}^\rho) + \sum_{i \in \mathcal{I}^\infty} \nu_i^\rho \nabla g_i(\mathbf{x}^\rho) = \mathbf{0}. \quad (46)$$

Since the MFCQ holds at \mathbf{x}^ρ , it can be verified that both $\boldsymbol{\lambda}^\rho$ and $\boldsymbol{\nu}^\rho$ must be bounded. Suppose not. Let

$$\bar{\boldsymbol{\lambda}} = \lim_{\rho \rightarrow \infty} \frac{\boldsymbol{\lambda}^\rho}{\|\boldsymbol{\lambda}^\rho\|_2 + \|\boldsymbol{\nu}^\rho\|_2}, \quad (47)$$

$$\bar{\boldsymbol{\nu}} = \lim_{\rho \rightarrow \infty} \frac{\boldsymbol{\nu}^\rho}{\|\boldsymbol{\lambda}^\rho\|_2 + \|\boldsymbol{\nu}^\rho\|_2} \neq \mathbf{0} (\geq \mathbf{0}). \quad (48)$$

Then, from (46) and by the fact that $\nabla f(\mathbf{x}^\rho)$ is bounded, we have

$$\sum_{j=1}^N \bar{\lambda}_j \nabla h_j(\mathbf{x}^\infty) + \sum_{i \in \mathcal{I}^\infty} \bar{\nu}_i \nabla g_i(\mathbf{x}^\infty) = \mathbf{0}. \quad (49)$$

However, by multiplying the LHS term of (49) with \mathbf{d}^∞ and by (40) and (41), we obtain

$$\left\langle \sum_{j=1}^N \bar{\lambda}_j \nabla h_j(\mathbf{x}^\infty) + \sum_{i \in \mathcal{I}^\infty} \bar{\nu}_i \nabla g_i(\mathbf{x}^\infty), \mathbf{d}^\infty \right\rangle < 0. \quad (50)$$

which is a contradiction with (49). Thus, by taking $\rho \rightarrow \infty$ in (46), we have for some $\boldsymbol{\lambda}^\infty$ and $\boldsymbol{\nu}^\infty$

$$\nabla f(\mathbf{x}^\infty) + \sum_{j=1}^N \lambda_j^\infty \nabla h_j(\mathbf{x}^\infty) + \sum_{i \in \mathcal{I}^\infty} \nu_i^\infty \nabla g_i(\mathbf{x}^\infty) = \mathbf{0}. \quad (51)$$

Again, by the Farkas lemma, we have

$$\begin{aligned} \langle \nabla f(\mathbf{x}^\infty), \mathbf{d} \rangle &\geq 0, \\ \forall \mathbf{d} \in \left\{ \mathbf{d} \in \mathbb{R}^n \mid \begin{array}{l} \langle \nabla h_j(\mathbf{x}^\infty), \mathbf{d} \rangle = 0, \quad \forall j \in \mathcal{N}, \\ \langle \nabla g_i(\mathbf{x}^\infty), \mathbf{d} \rangle \leq 0, \quad i \in \mathcal{I}^\infty \end{array} \right\}, \end{aligned} \quad (52)$$

which implies that

$$\langle \nabla f(\mathbf{x}^\infty), \mathbf{d} \rangle \geq 0, \quad \forall \mathbf{d} \in \mathcal{T}_{\mathcal{X}}(\mathbf{x}^\infty). \quad (53)$$

By (53) and by (A1), we conclude that \mathbf{x}^∞ is a stationary solution of problem (38). \blacksquare

Appendix D. Proof of Theorem 2

Proof of (a): Denote $\phi(\mathbf{h}_j) \triangleq \mathbf{1}^T \mathbf{h}_j - \|\mathbf{h}_j\|_\infty$. Since $(\mathbf{W}^\rho, \mathbf{H}^\rho)$ is a d-stationary point of (20), we have

$$\langle \nabla_{\mathbf{H}} F(\mathbf{W}^\rho, \mathbf{H}^\rho), \mathbf{D} \rangle + \rho \sum_{j=1}^N \phi'(\mathbf{h}_j^\rho; \mathbf{d}_j) \geq 0, \forall \mathbf{D} \in \mathcal{T}_{\mathcal{H}^+}(\mathbf{H}^\rho), \quad (54)$$

where $\mathcal{T}_{\mathcal{H}^+}(\mathbf{H}^\rho)$ is given in (36). Because

$$\phi'(\mathbf{h}_j^\rho; \mathbf{d}_j) = \mathbf{1}^T \mathbf{d}_j - \max_{\mathbf{g} \in \partial \|\mathbf{h}_j^\rho\|_\infty} \mathbf{g}^T \mathbf{d}_j, \quad (55)$$

and $\mathbf{e}_{i_j^*} \in \partial \|\mathbf{h}_j^\rho\|_\infty$, where $i_j^* \in \arg \max_{i=1, \dots, K} [\mathbf{H}^\rho]_{i,j}$, condition (54) implies

$$\langle \nabla_{\mathbf{H}} F(\mathbf{W}^\rho, \mathbf{H}^\rho), \mathbf{D} \rangle + \rho \sum_{j=1}^N \left(\mathbf{1}^T \mathbf{d}_j - \mathbf{e}_{i_j^*}^T \mathbf{d}_j \right) \geq 0, \forall \mathbf{D} \in \mathcal{T}_{\mathcal{H}^+}(\mathbf{H}^\rho). \quad (56)$$

On the other hand, we can upper bound

$$\begin{aligned} \langle \nabla_{\mathbf{H}} F(\mathbf{W}^\rho, \mathbf{H}^\rho), \mathbf{D} \rangle &= \langle 2(\mathbf{W}^\rho)^T (\mathbf{W}^\rho \mathbf{H}^\rho - \mathbf{X}) + \nu \mathbf{H}^\rho, \mathbf{D} \rangle \\ &\leq \|2(\mathbf{W}^\rho)^T (\mathbf{W}^\rho \mathbf{H}^\rho - \mathbf{X}) + \nu \mathbf{H}^\rho\|_F \|\mathbf{D}\|_F \\ &\leq \|2(\mathbf{W}^\rho)^T (\mathbf{W}^\rho \mathbf{H}^\rho - \mathbf{X}) + \nu \mathbf{H}^\rho\|_F \|\mathbf{D}\|_1 \\ &\triangleq \rho^* \|\mathbf{D}\|_1. \end{aligned} \quad (57)$$

By substituting (57) into (56), we obtain

$$\rho^* \|\mathbf{D}\|_1 + \rho \sum_{j=1}^N \left(\mathbf{1}^T \mathbf{d}_j - \mathbf{e}_{i_j^*}^T \mathbf{d}_j \right) \geq 0, \forall \mathbf{D} \in \mathcal{T}_{\mathcal{H}^+}(\mathbf{H}^\rho). \quad (58)$$

We argue that $\phi(\mathbf{h}_j^\rho) = 0$ for all $j \in \mathcal{N}$ if $\rho > \rho^*$. Suppose not. Then, there exists an index $j' \in \mathcal{N}$ such that $\phi(\mathbf{h}_{j'}^\rho) > 0$. Let us choose a tangent $\mathbf{D}^\rho \in \mathcal{T}_{\mathcal{H}^+}(\mathbf{H}^\rho)$ as follows

$$[\mathbf{D}^\rho]_{i,j} = \begin{cases} -1, & \text{for } j = j', [\mathbf{H}^\rho]_{i,j} > 0 \text{ and } i \neq i_j^*, \\ 0, & \text{otherwise.} \end{cases} \quad (59)$$

Substituting (59) into (58) gives rise to

$$(\rho^* - \rho) \|\mathbf{d}_{j'}^\rho\|_1 \geq 0, \quad (60)$$

which is a contradiction since $\rho > \rho^*$. Thus $\phi(\mathbf{h}_j^\rho) = 0, \forall j \in \mathcal{N}$, must hold if $\rho > \rho^*$.

Proof of (b): The statement can actually be obtained by applying (Nocedal and Wright, 2006, Theorem 17.4). Here we provide a proof for (20). Since $(\mathbf{W}^\rho, \mathbf{H}^\rho)$ is a d-stationary point of (20), we have

$$\begin{aligned} \langle \nabla_{\mathbf{H}} F(\mathbf{W}^\rho, \mathbf{H}^\rho), \mathbf{D} \rangle + \langle \nabla_{\mathbf{W}} F(\mathbf{W}^\rho, \mathbf{H}^\rho), \mathbf{S} \rangle + \rho \sum_{j=1}^N \phi'(\mathbf{h}_j^\rho; \mathbf{d}_j) &\geq 0, \\ \forall \mathbf{D} \in \mathcal{T}_{\mathcal{H}^+}(\mathbf{H}^\rho), \mathbf{S} \in \mathcal{T}_{\mathcal{W}^+}(\mathbf{W}^\rho), & \end{aligned} \quad (61)$$

where $\mathcal{T}_{\mathcal{H}^+}(\mathbf{H}^\rho)$ and $\mathcal{T}_{\mathcal{W}^+}(\mathbf{W}^\rho)$ are defined in (36). From Theorem 2(a), $(\mathbf{W}^\rho, \mathbf{H}^\rho)$ is feasible to $\mathcal{H}_{1,\infty}^1$ in (8c) for $\rho > \rho^*$. Thus, the tangent cone of $\mathcal{H}_{1,\infty}^1$ at \mathbf{H}^ρ is given by

$$\mathcal{T}_{\mathcal{H}_{1,\infty}^1}(\mathbf{H}^\rho) = \left\{ \mathbf{D} \mid \begin{array}{l} \mathbf{d}_j = \mathbf{e}_l, \forall l \in \mathcal{N}, \text{ if } \|\mathbf{h}_j^\rho\|_2 = 0; \\ [\mathbf{D}]_{i,j} = \pm 1, \text{ if } [\mathbf{H}^\rho]_{i,j} > 0; \\ [\mathbf{D}]_{i,j} = 0, \text{ otherwise.} \end{array} \right\} \quad (62)$$

$$\subset \mathcal{T}_{\mathcal{H}^+}(\mathbf{H}^\rho). \quad (63)$$

Besides, one can verify that for all $\mathbf{D} \in \mathcal{T}_{\mathcal{H}_{1,\infty}^1}(\mathbf{H}^\rho)$,

$$\phi'(\mathbf{h}_j^\rho; \mathbf{d}_j) = \mathbf{1}^T \mathbf{d}_j - \max_{\mathbf{g} \in \partial(\|\mathbf{h}_j^\rho\|_\infty)} \mathbf{g}^T \mathbf{d}_j = 0, \forall j \in \mathcal{N}. \quad (64)$$

Therefore, by applying (63) and (64) to (61), we obtain

$$\langle \nabla_{\mathbf{H}} F(\mathbf{W}^\rho, \mathbf{H}^\rho), \mathbf{D} \rangle + \langle \nabla_{\mathbf{W}} F(\mathbf{W}^\rho, \mathbf{H}^\rho), \mathbf{S} \rangle \geq 0, \forall \mathbf{D} \in \mathcal{T}_{\mathcal{H}_{1,\infty}^1}(\mathbf{H}^\rho), \mathbf{S} \in \mathcal{T}_{\mathcal{W}}(\mathbf{W}^\rho), \quad (65)$$

which says that $(\mathbf{W}^\rho, \mathbf{H}^\rho)$ is a B-stationary point to (8). \blacksquare

Appendix E. Descent Property of Algorithm 3

We show that the update of \mathbf{H} in Algorithm 3

$$\mathbf{H}^{k+1} = \max \left\{ \mathbf{H}^k - \frac{1}{t^k} (\nabla_{\mathbf{H}} \tilde{F}(\mathbf{W}^k, \mathbf{H}^k) - \rho \mathbf{G}^k), 0 \right\}, \quad (66)$$

where $t^k > \frac{L_{\tilde{F}}(\mathbf{W}^k)}{2}$, is a descent update for the objective function $F_\rho(\mathbf{W}^k, \mathbf{H})$, i.e., $F_\rho(\mathbf{W}^k, \mathbf{H}^{k+1}) < F_\rho(\mathbf{W}^k, \mathbf{H}^k)$.

Note that (66) is equivalent to

$$\mathbf{H}^{k+1} = \arg \min_{\mathbf{H} \in \mathcal{H}^+} \left\{ \langle \nabla_{\mathbf{H}} \tilde{F}(\mathbf{W}^k, \mathbf{H}^k) - \rho \mathbf{G}^k, \mathbf{H} - \mathbf{H}^k \rangle + \frac{t^k}{2} \|\mathbf{H} - \mathbf{H}^k\|_F^2 \right\}. \quad (67)$$

By the optimality condition of (67), we obtain

$$\langle \nabla_{\mathbf{H}} \tilde{F}(\mathbf{W}^k, \mathbf{H}^k) - \rho \mathbf{G}^k + t^k (\mathbf{H}^{k+1} - \mathbf{H}^k), \mathbf{H} - \mathbf{H}^{k+1} \rangle \geq 0, \forall \mathbf{H} \in \mathcal{H}^+. \quad (68)$$

By letting $\mathbf{H} = \mathbf{H}^k$, it gives rise to

$$\langle \nabla_{\mathbf{H}} \tilde{F}(\mathbf{W}^k, \mathbf{H}^k) - \rho \mathbf{G}^k, \mathbf{H}^{k+1} - \mathbf{H}^k \rangle + t^k \|\mathbf{H}^{k+1} - \mathbf{H}^k\|_2^2 \leq 0. \quad (69)$$

Since $\tilde{F}(\mathbf{W}^k, \mathbf{H})$ is gradient Lipschitz continuous, it satisfies

$$\tilde{F}(\mathbf{W}^k, \mathbf{H}^{k+1}) \leq \tilde{F}(\mathbf{W}^k, \mathbf{H}^k) + \langle \nabla_{\mathbf{H}} \tilde{F}(\mathbf{W}^k, \mathbf{H}^k), \mathbf{H}^{k+1} - \mathbf{H}^k \rangle + \frac{L_{\tilde{F}}(\mathbf{W}^k)}{2} \|\mathbf{H}^{k+1} - \mathbf{H}^k\|_F^2. \quad (70)$$

Substituting (69) into (70) gives rise to

$$\tilde{F}(\mathbf{W}^k, \mathbf{H}^{k+1}) - \langle \mathbf{G}^k, \mathbf{H}^{k+1} - \mathbf{H}^k \rangle \leq \tilde{F}(\mathbf{W}^k, \mathbf{H}^k) - \left(t^k - \frac{L_{\tilde{F}}(\mathbf{W}^k)}{2} \right) \|\mathbf{H}^{k+1} - \mathbf{H}^k\|_F^2. \quad (71)$$

As $\sum_{j=1}^N \|\mathbf{h}_j\|_\infty$ is convex, we have

$$\sum_{j=1}^N \|\mathbf{h}_j^{k+1}\|_\infty \geq \sum_{j=1}^N \|\mathbf{h}_j^k\|_\infty + \langle \mathbf{G}^k, \mathbf{H}^{k+1} - \mathbf{H}^k \rangle, \quad (72)$$

which together with (71) and $t^k > \frac{L_{\bar{F}}(\mathbf{W}^k)}{2}$ lead to the desired result of $F_\rho(\mathbf{W}^k, \mathbf{H}^{k+1}) < F_\rho(\mathbf{W}^k, \mathbf{H}^k)$. \blacksquare

References

- C. C. Aggarwal and C. K. Reddy. *Data Clustering: Algorithms and Applications*. Chapman & Hall/CRC Press, Boca Raton, FI, USA, 2013.
- D. Arthur and S. Vassilvitskii. K-means++: The advantages of careful seeding. In *Proc. SODA*, pages 1027–1035, Philadelphia, PA, USA, Jan. 07-08 2007.
- M. Asteris, D. Papailiopoulos, and A. G. Dimakis. Orthogonal NMF through subspace exploration. In *Proc. NIPS*, pages 343–351, Canada, Dec. 07-12 2015.
- M.-F. F Balcan, S. Ehrlich, and Y. Liang. Distributed k-means and k-median clustering on general topologies. In *Proc. NIPS*, pages 1995–2003, Lake Tahoe, Nevada, Dec. 05-10 2013.
- C. Bauckhage. K-means clustering is matrix factorization. *arXiv preprint arXiv:1512.07548*, 2015.
- D. P. Bertsekas. *Nonlinear Programming, 2nd Edition*. Athena Scientific, Belmont, Massachusetts, 1999.
- A. Bhaskara and M. Wijewardena. Distributed clustering via LSH based data clustering. In *Proc. NIPS*, pages 570–579, Stockholmsmassan, Stockholm Sweden, Jul. 10-15 2018.
- J. Bolte, S. Sabach, and M. Teboulle. Proximal alternating linearized minimization for non-convex and non-smooth problems. *Math Program.*, 146, no. 1:459–494, Aug. 2014.
- J.-P. Brunet, P. Tamayo, T. R. Golub, and J. P. Mesirov. Metagenes and molecular pattern discovery using matrix factorization. In *Proc. Natl. Acad. Sci. USA*, pages 4164–4169, Mar. 23 2004.
- D. Cai, X. He, and J. Han. Locally consistent concept factorization for document clustering. *IEEE Trans. Knowl. Data Eng.*, 23, no. 6:902–913, Jun. 2011.
- C.-S. Chang, W. Liao, Y.-S. Chen, and L.H. Liou. A mathematic theory for clustering in metric spaces. *IEEE Transactions on Network Science and Engineering*, 3, no. 1:2–16, 2016.
- S. Choi. Algorithms for orthogonal non-negative matrix factorization. In *Proc. IEEE IJCNN*, pages 1828–1832, Hong Kong, China, Jun. 01-08 2008.

- J. Das, P. Mukherjee, S. Majumder, and P. Gupta. Clustering-based recommender system using principles of voting theory. In *Proc. IEEE IC3I*, pages 230–235, Mysore, India, Nov. 27-29 2014.
- C. Ding, T. Li, W. Peng, and H. Park. Orthogonal non-negative matrix t-factorizations for clustering. In *Proc. ACM KDD*, pages 20–23, Philadelphia, PA, USA, Aug. 20-23 2006.
- C. Ding, T. Li, and M. I. Jordan. Convex and semi-nonnegative matrix factorizations. *IEEE TPAMI*, 32, no. 1:45–55, Jan. 2010.
- H. Ding, Y. Liu, L. Huang, and J. Li. K-means clustering with distributed dimensions. In *Proc. ICML*, pages 1339–1348, New York, USA, Jun. 19-24 2016.
- F. Facchinei and J.-S. Pang. *Finite-Dimensional Variational Inequalities and Complementarity Problems, Vol. I*. Springer-Verlag, New York Berlin Heidelberg, 2003.
- O. Fercoq and P. Richtarik. Accelerated, parallel, and proximal coordinate descent. *SIAM J. Optim.*, 25, no. 4:1997–2023, Jul. 2015.
- C. Fevotte and J. Idier. Algorithms for nonnegative matrix factorization with the β -divergence. *Neural Computation*, 23, no. 9:2421–2456, Sept 2011.
- M. Goesele, S. Roth, A. Kuijper, B. Schiele, and K. Schindler. Efficient object detection using orthogonal NMF descriptor hierarchies. In *Proc. DAGM*, pages 212–221, Darmstadt, Germany, Sept. 22-24 2010.
- Y. Kim, T.-K. Kim, Y. Kim, J. Yoo, S. You, I. Lee, G. Carlson, L. Hood, S. Choi, and D. Hwang. Principal network analysis: identification of subnetworks representing major dynamics using gene expression data. *Bioinformatics*, 27, no. 3:391–398, Dec. 2010.
- K. Kimura, Y. Tanaka, and M. Kudo. A fast hierarchical alternating least squares algorithm for orthogonal non-negative matrix factorization. In *Proc. ACML*, pages 129–141, Nha Trang City, Vietnam, Nov. 26-28 2015.
- Y. LeCun, C. Cortes, and C. Burges. The mnist database. URL <http://yann.lecun.com/exdb/mnist/>.
- D. D. Lee and H. S. Seung. Algorithms for non-negative matrix factorization. In *Proc. NIPS*, pages 556–562, Denver, CO, USA, Dec. 2000.
- Q. Lin, Z. Lu, and X. Lin. An accelerated proximal coordinate gradient method. In *Proc. NIPS*, pages 3059–3067, Montreal, Canada, Dec. 08-13 2014.
- Z. Liu, Z. Yang, and E. Oja. Selecting beta-divergence for nonnegative matrix factorization by score matching. In *Proc. ICANN*, pages 419–426, Lausanne, Switzerland, Sept. 11-14 2012.
- S. Lloyd. Least squares quantization in PCM. *IEEE Trans. Info. Theory*, 28(2):129–137, Mar. 1982.

- U. Luxburg. A tutorial on spectral clustering. *Statistics and Computing*, 17, no. 4:395–416, Dec. 2007.
- H. Mansour, S. Rane, P. T. Boufounos, and A. Vetro. Video querying via compact descriptors of visually salient objects. In *Proc. IEEE ICIP*, pages 2789–2793, Paris, France, Oct. 27-30 2014.
- A. Mirzal. Nonparametric orthogonal NMF and its application in cancer clustering. In *Proc. DaEng*, pages 177–184, Kuala Lumpur, Malaysia, Dec. 15 2013.
- J. Nocedal and S. J. Wright. *Numerical Optimization*. Springer Series in Operations Research and Financial Engineering, Jan. 1 2006.
- J.-S. Pang, M. Razaviyayn, and A. Alvarado. Computing B-Stationary points of non-smooth dc programs. *Math. Ope. Res.*, 42, no. 1:95–118, Jan. 2017.
- D. N. Phan, H. M. Le, and H. A. Le Thi. Accelerated difference of convex functions algorithm and its application to sparse binary logistic regression. In *Proc. IJCAI*, pages 1369–1375, Stockholm, Sweden, Jul. 13-19 2018.
- F. Pompili, N. Gillis, P. A. Absil, and F. Glineur. Two algorithms for orthogonal non-negative matrix factorization with application to clustering. *Neurocomputing*, 141, no. 2: 15–25, Oct. 2014.
- S. Renaud-Deputter, T. Xiong, and S. Wang. Combining collaborative filtering and clustering for implicit recommender system. In *Proc. IEEE AIAN*, pages 748–755, Barcelona, Spain, Mar. 25-28 2013.
- M. Strazar, M. Zitnik, B. Zupan, J. Ule, and T. Curk. Orthogonal matrix factorization enables integrative analysis of multiple rna binding proteins. *Bioinformatics*, 32, no. 10: 1527–1535, Jan. 2016.
- S. Theodoridis and K. Koutroumbas. *Pattern Recognition*. Academic Press, Burlington, MA, 2008.
- A. C. Turkmen. A review of non-negative matrix factorization methods for clustering. *CoRR*, abs/1507.03194, 2015.
- S. Wang, P. Wu, M. Zhou, T.-H. Chang, and S. Wu. Cell subclass identification in single-cell RNA-sequencing data using orthogonal non-negative matrix factorization. In *Proc. IEEE ICASSP*, pages 876–880, Calgary, Canada, Apr. 15-20 2018.
- S. Wang, T.-H. Chang, Y. Cui, and J.-S. Pang. Clustering by orthogonal non-negative matrix factorization: A sequential non-convex penalty approach. In *Proc. IEEE ICASSP*, pages 5576–5580, Brighton, UK, May 12-17 2019.
- J. Xie, R. Girshick, and A. Farhadi. Unsupervised deep embedding for clustering analysis. In *Proc. ICML*, pages 478–487, New York, NY, USA, Jun. 19-24 2016.
- B. Yang, X. Fu, and N. D. Sidiropoulos. Learning from hidden traits: joint factor analysis and latent clustering. *IEEE Trans. Signal Process.*, 65:256–269, Jan. 2017a.

- B. Yang, X. Fu, N. D. Sidiropoulos, and M. Hong. Towards K-means-friendly spaces: simultaneous deep learning and clustering. In *Proc. ICML*, pages 3861–3870, Sydney, Australia, Aug. 06-11 2017b.
- K. Y. Yeung and W. L. Ruzzo. Details of the adjusted rand index and clustering algorithms, supplement to the paper an empirical study on principal component analysis for clustering gene expression data. *Bioinformatics*, 17, no. 9:763–774, May 2001.
- J. Yoo and S. Choi. Non-negative matrix factorization with orthogonality constraints. *J. Comp. Sci. Eng.*, 4, no. 2:97–109, May 2010.
- C.-H. Zheng, D.-S. Huang, L. Zhang, and X.-Z. Kong. Tumor clustering using nonnegative matrix factorization with gene selection. *IEEE. Transactions on Information Technology in Biomedicine*, 13, no. 4:599–607, Jul. 2009.